OPEN ACCESS

ORIGINAL ARTICLE

OCT1 is a determinant of synbindin-related ERK signalling with independent prognostic significance in gastric cancer

Jin Qian,[1] Xuan Kong,[1] Niantao Deng,[2] Patrick Tan,[2,3] Haoyan Chen,[1] Jilin Wang,[1] Zhaoli Li,[4] Ye Hu,[1] Weiping Zou,[5] Jie Xu,[1] Jing-Yuan Fang[1]

▶ Additional material is published online only. To view please visit the journal online (http://dx.doi.org/10.1136/gutjnl-2013-306584).

[1]State Key Laboratory of Oncogenes and Related Genes, Division of Gastroenterology and Hepatology, Renji Hospital, School of Medicine, Shanghai Jiao Tong University, Shanghai Cancer Institute, Shanghai Institute of Digestive Disease, Shanghai, China
[2]Cancer and Stem Cell Biology Program, Duke-NUS Graduate Medical School, Singapore, Singapore
[3]Cancer Therapeutics and Stratified Oncology, Genome Institute of Singapore, Singapore, Singapore
[4]Harbin Veterinary Research Institute, Chinese Academy of Agricultural Sciences, Harbin, China
[5]Department of Surgery, University of Michigan, Ann Arbor, Michigan, USA

Correspondence to
Dr Jing-Yuan Fang; jingyuanfang@yahoo.com
and Dr Jie Xu; jiexu@yahoo.com

Received 11 December 2013
Accepted 17 March 2014
Published Online First 9 April 2014

To cite: Qian J, Kong X, Deng N, *et al*. *Gut* 2015;**64**:37–48.

ABSTRACT

Objective Octamer transcription factor 1 (OCT1) was found to be expressed in intestinal metaplasia and gastric cancer (GC), but the exact roles of OCT1 in GC remain unclear. The objective of this study was to determine the functional and prognostic implications of OCT1 in GC.

Design Expression of OCT1 was examined in paired normal and cancerous gastric tissues and the prognostic significance of OCT1 was analysed by univariate and multivariate survival analyses. The functions of OCT1 on synbindin expression and extracellular signal-regulated kinase (ERK) phosphorylation were studied in vitro and in xenograft mouse models.

Results The OCT1 gene is recurrently amplified and upregulated in GC. OCT1 overexpression and amplification are associated with poor survival in patients with GC and the prognostic significance was confirmed by independent patient cohorts. Combining OCT1 overexpression with American Joint Committee on Cancer staging improved the prediction of survival in patients with GC. High expression of OCT1 associates with activation of the ERK mitogen-activated protein kinase signalling pathway in GC tissues. OCT1 functions by transactivating synbindin, which binds to ERK DEF domain and facilitates ERK phosphorylation by MEK. OCT1-synbindin signalling results in the activation of ERK substrates ELK1 and RSK, leading to increased cell proliferation and invasion. Immunofluorescent study of human GC tissue samples revealed strong association between OCT1 protein level and synbindin expression/ERK phosphorylation. Upregulation of OCT1 in mouse xenograft models induced synbindin expression and ERK activation, leading to accelerated tumour growth in vivo.

Conclusions OCT1 is a driver of synbindin-mediated ERK signalling and a promising marker for the prognosis and molecular subtyping of GC.

Significance of this study

What is already known on this subject?

- Octamer transcription factor 1 (OCT1) is a homologue of OCT4 pluripotency factor, and it is expressed in intestinal metaplasia foci and in gastric cancers (GCs).
- The mitogen-activated protein kinase (MAPK) pathway is one of the most frequently altered signalling pathways in GC.
- Synbindin is a spatial regulator of the extracellular signal-regulated kinases (ERK)/MAPK signalling pathway.

What are the new findings?

- The OCT1 gene is recurrently amplified in the genome of GC, and OCT1 amplification displays mutual exclusivity with KRAS and FGFR2 genes in the receptor tyrosine kinase (RTK) pathway.
- OCT1 gene amplification and upregulation are associated with poor survival of patients with GC, and the association is supported by independent datasets.
- OCT1 transactivates synbindin, which binds to the ERK DEF domain and potentiates ERK phosphorylation by MEK1, leading to activation of the ERK substrates ELK1 and RSK. The expression of OCT1 strongly correlates with the levels of synbindin and ERK phosphorylation in GC tissues.
- OCT1 upregulation suppresses apoptosis and enhances proliferation and invasion of GC cells. Knockdown of synbindin expression blocked the pro-malignant effects of OCT1.
- In xenograft tumour models, OCT1 substantially promoted synbindin expression and ERK activation, leading to accelerated tumour growth in vivo.

INTRODUCTION

Stomach adenocarcinoma, or gastric cancer (GC), is the fourth most common cancer and the second highest cause of cancer-related mortality worldwide.[1] The prognosis of patients with GC continues to be dismal, despite improving surgical and adjuvant treatment approaches, with a 5-year overall survival less than 25%.[2] It is of great clinical importance to identify genes that control the severity of GC and present predictive value for prognosis.[3 4] In a systematic study of molecular signatures in GC, mitogen-activated protein kinase (MAPK) was found as the most frequently activated pathway in this deadly disease.[5] In support of this, several components of the receptor tyrosine kinase (RTK)/RAS/MAPK pathway were found to be frequently amplified in GC.[6 7] Since MAPK signalling is also controlled by spatiotemporal regulatory mechanisms,[8 9] it is of interest to test if alternative pathways may contribute to MAPK deregulation in GC.

Significance of this study

How might it impact on clinical practice in the foreseeable future?

- Amplification of OCT1 contributes to ERK/MAPK activation, and it may join other components in the RTK pathway to mark patients with GC who are potentially treatable by RTK/RAS directed therapies (up to 46% of the GC population by simplified estimation).
- OCT1 is an independent prognostic factor in GC, and combining OCT1 expression with American Joint Committee on Cancer staging could further improve the prediction of patient survival. OCT1 gene amplification and upregulation can be used as a promising biomarker for the prognosis of GC.

Octamer transcription factor 1 (OCT1) (POU2F1) belongs to the POU homeodomain family of transcription factors.[10] This protein activates or represses the transcription of various genes, such as the immunoglobulin genes in B cells[11] and several interleukins.[12] Accumulating data suggest that OCT1 may contribute to the malignant transformation process, and loss of OCT1 inhibits oncogenic transformation in mouse embryonic fibroblasts and tumourigenicity in p53-deficient mice.[13] Moreover, OCT1 is believed to facilitate the tumourigenesis of pancreatic and intestinal cancer cells through transactivating the CDX2 gene.[14] Interestingly, OCT1 has been reported to be positive in 87% of intestinal metaplasia foci (a preneoplastic lesion) and in 74% of gastric carcinomas in one series.[15] Nonetheless, in GC cells OCT1 was found without the ability to transactivate CDX2, although it could bind to the CDX2 promoter.[15] Despite recent efforts to understand the activities of OCT1 as a transcriptional factor,[16] little is known about the roles of OCT1 in gastric carcinogenesis and it remains unclear whether OCT1 expression may associate with any clinicopathological features of GC.

Here we report OCT1 as an independent prognostic marker for GC and it regulates the extracellular signal-regulated kinase (ERK) MAPK signalling by transactivating synbindin. Synbindin is a core subunit of the trafficking protein particle complex and it is involved in the targeting and fusion of vesicles from endoplasmic reticulum to Golgi apparatus.[17] We previously found that synbindin functions as a scaffold protein that binds to MEK and ERK2, facilitating MEK-dependent phosphorylation and activation of ERK2 on the Golgi.[9] In this study, we further show that OCT1 binds to and transactivates the promoter of synbindin, thereby inducing synbindin-mediated activation of ERK signalling in GC. We obtained in vitro and in vivo data supporting the major regulatory effects of OCT1 on ERK signalling and the aggressive behaviours of GC cells. Importantly, we demonstrate that OCT1 amplification and upregulation associate with poor outcome in patients with GC. By these approaches we aim to elucidate the functional and prognostic implications of OCT1 in GC.

MATERIALS AND METHODS

Immunofluorescence

Tissue specimens were from patients (89 cases for immunofluorescence and 10 for fluorescent in situ hybridization (FISH)) who underwent surgery at the Shanghai Renji Hospital from July 2003 to January 2009. The protocol had the approval of the Ethics Committee of the Shanghai Jiao-Tong University School of Medicine, Renji Hospital, and the research was carried out according to the provisions of the Helsinki Declaration of 1975. Written informed consent was obtained from all participants involved in the study, and clinical information was collected with Institutional Review Board approval. Meanwhile, 89 specimens of adjacent tissues were taken from these patients as the paired controls. The tissue sections were deparaffinised in xylene and rehydrated using a graded series of ethanol. All slides were treated with NaBH4 to suppress autofluorescence of tissues. The expression levels of OCT1 and synbindin were probed with the primary antibodies (OCT1, dilution 1:40; synbindin, dilution 1:40) according to the manufacturer's instructions. Secondary antibodies (Alexa488-anti-mouse and Alexa546-anti-rabbit) were used to label synbindin and OCT1, respectively. Protein expression was quantified based on staining intensity.

Fluorescent in situ hybridisation

The FISH protocol to detect gene copy number variation (CNV) in formalin-fixed paraffin embedded tissues has been described in detail previously.[18] Briefly, the OCT1 DNA probes were labelled using spectrum green and control probes in spectrum orange (centromeric CEP probe for chromosomes 1) (Abbott Molecular Inc, Des Plaines, Illinois, USA). Hybridised slides were counterstained with DAPI and analysed using Zeiss LSM710 confocal microscope (Carl Zeiss, Regensburg, Germany).

Additional materials and methods including chromatin immunoprecipitation (ChIP), cell viability and invasion assays, flow cytometry, gene set enrichment analysis (GSEA), CNV analysis, TF binding identification, Western blotting, and in vivo experiments can be found in the online supplementary information.

RESULTS

OCT1 expression and CNV in GC

We first investigated OCT1 expression level in gastric adenocarcinoma (90 cases) and their adjacent normal controls by immunofluorescence histochemistry. As a result, OCT1 was weakly or moderately detected in normal gastric mucosa (figure 1A), but its expression level was substantially increased in GC cells ($p<0.0001$, figure 1B,C). Notably, OCT1 was strongly positive in the nucleus of GC cells, suggesting its active status as a transcriptional factor (figure 1D). In addition, we detected increased OCT1 expression in gastric tissues with intestinal metaplasia (see online supplementary figure S1A), which confirmed previous findings.[15]

Further, we analysed the CNV of OCT1 in GC tissues using data from The Cancer Genome Atlas (TCGA) GC cohort,[19] the Singapore[6] and the VUMC cohorts.[20] The GISTIC 2.0 package was employed to identify focal alteration events based on Affymetrix SNP6 microarray data (TCGA and Singapore datasets), while the CGHCall algorithm was used to analyse aCGH data (VUMC dataset). The OCT1 (POU2F1) gene is located in a recurrently amplified region in chromosome 1 (see online supplementary figure S1B), with 31 of 305 patients (10.16%) showing focal amplification (q value <0.001) but only one patient with deletion (figure 1E). This result was confirmed by the Singapore GC patient cohort, which reported 18 in 193 patients with GC (9.33) with focal amplification of OCT1 gene (figure 1E). In fact, algorithms that identify focal and broad (q value<0.25) CNV events show much higher frequency of OCT1 amplifications, ranging from 22.2% (40 of 180 cases in VUMC cohort) to 32.1% (98 of 305 cases in TCGA cohort) (figure 1E, see online supplementary figure S1C–E). We

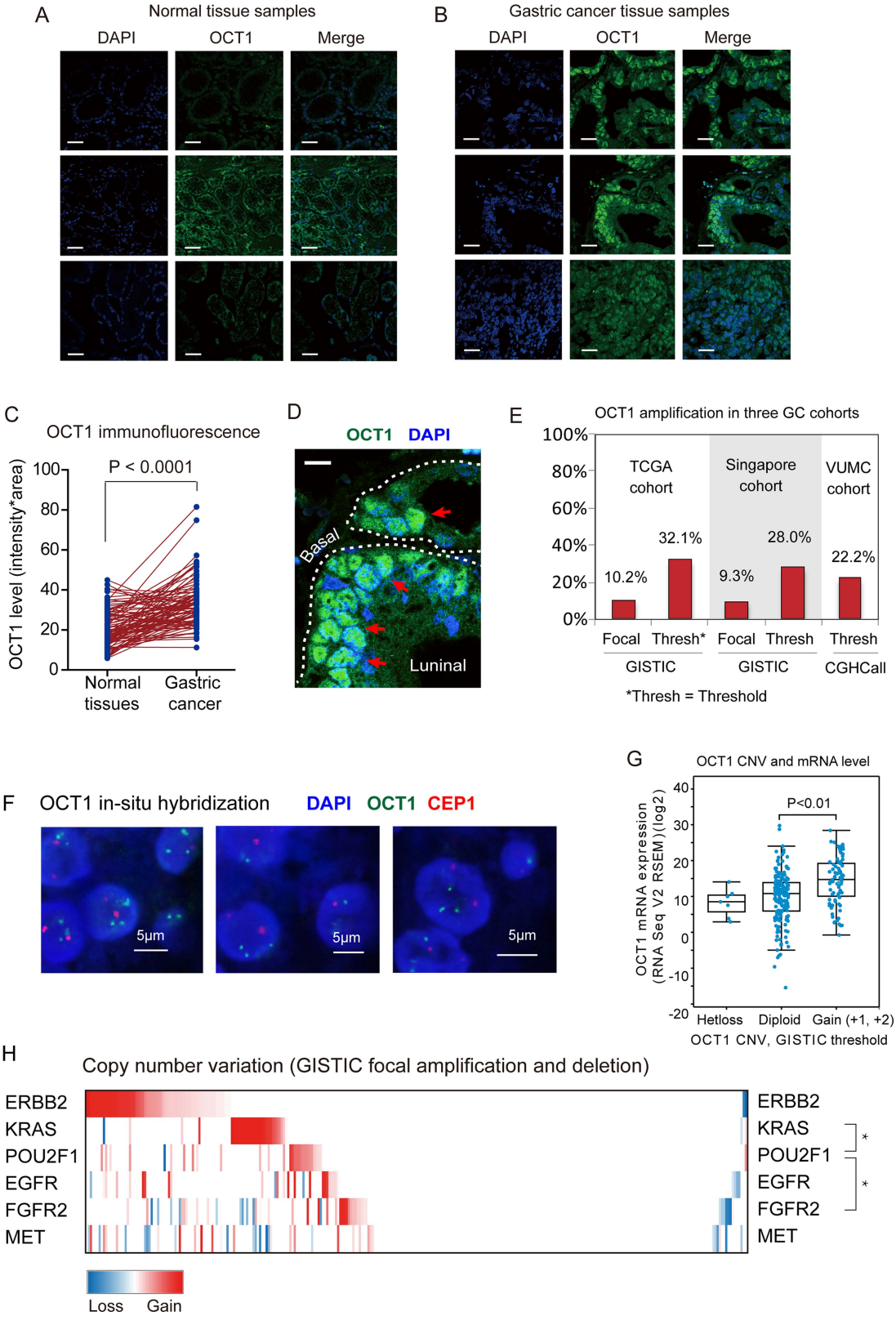

Figure 1 Amplification and overexpression of octamer transcription factor 1 (OCT1) gene in gastric cancer (GC). (A) Expression of OCT1 in normal gastric tissues as determined by immunofluorescence. Scale bars indicate 10μm in all panels. (B) Immunostain of OCT1 in gastric cancer tissues. (C) Statistical analysis of OCT1 expression in normal and GC tissues (P<0.0001, Mann Whitney test). (D) The immunofluorescent image shows OCT1 (in green) and cell nucleus (in blue)OCT1 is strongly expressed in the cell nucleus (red arrows). (E) The frequency of OCT1 amplification in three independent GC cohorts as indicated. (F) OCT1 genomic amplification confirmed by fluorescence in-situ hybridization (FISH) assay. Green signals indicate the OCT1 FISH probe, and red signals probe to centremore 1. Scale bars indicate 5μm in all panels. (G) OCT1 mRNA levels were significantly higher in samples with OCT1 gained CNA compared with the samples without CNV in the TCGA dataset (P<0.01, 2-sided t-test). (H) Relationship between the CNVs of OCT1 and frequently altered genes in Receptor tyrosine kinase (RTK) pathway. The mutual exclusivity between the CNVs of OCT1 (POU2F1) and other genes was determined by dimension reduction permutation (DRP) algorithm (*P<0.05).

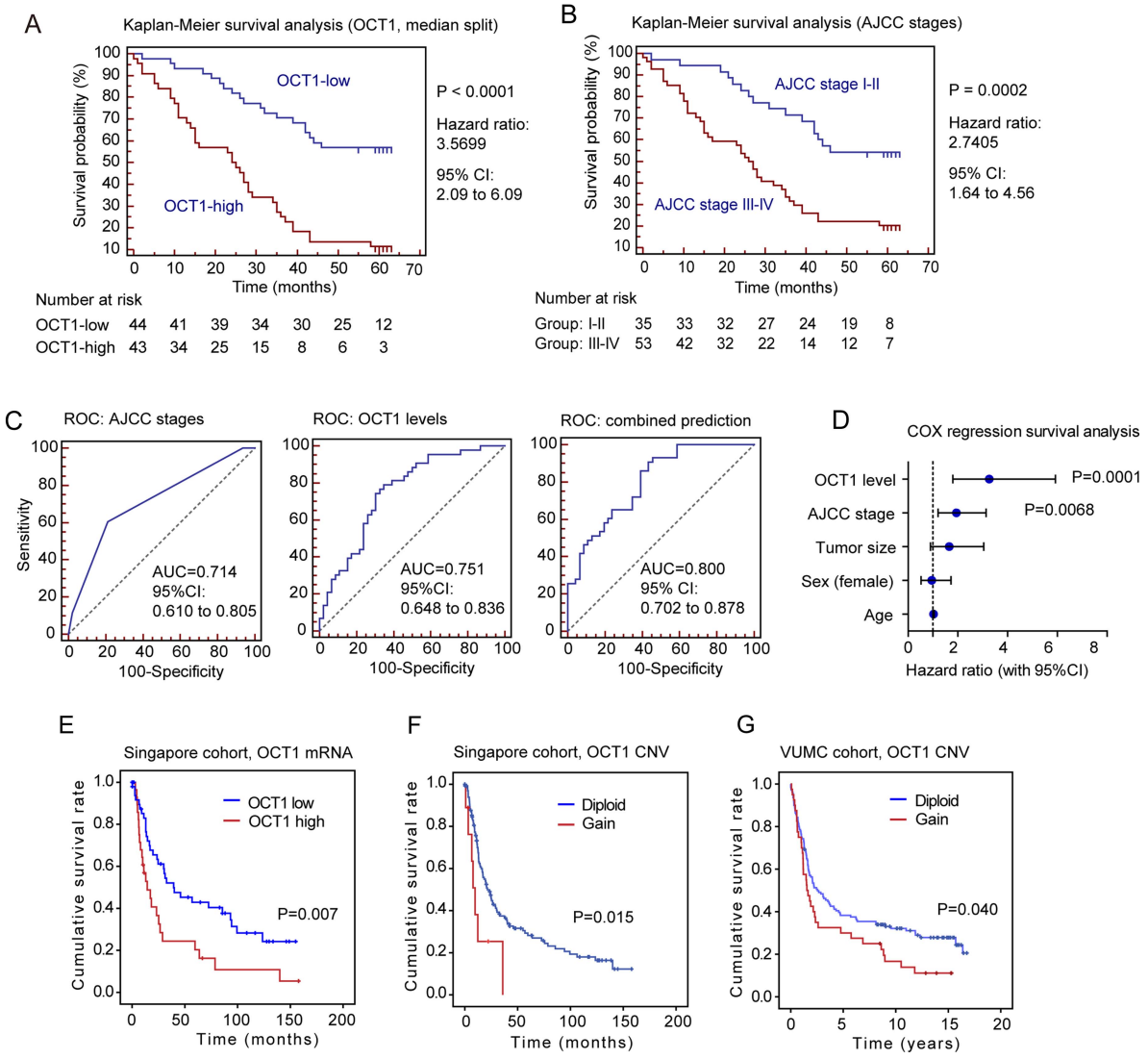

Figure 2 Octamer transcription factor 1 (OCT1) gene amplification and upregulation are associated with poor survival in patients with GC. (A) Kaplan-Meier survival analysis of GC patients stratified by OCT1 expression level (median split). (B) Kaplan-Meier survival analysis of GC patients with different AJCC tumor stages (I-II v.s. III-IV). (C) The receiver operating characteristic (ROC) curves for predicting patient survival using AJCC stage (left panel), OCT1 level (middle panel) or combination of two factors (right panel). The area under curve (AUC) and the corresponding 95% CI are shown in the plots. (D) Different factors (including OCT1, AJCC stage, tumor size, sex and age) were analyzed for their association with patient survival using Cox regression model. The hazard ratio and 95% confident interval (CI) are plotted for each factor. (E) The GC patients in the Singapore cohort were stratified according to OCT1 mRNA level (median split) and compared for the survival using Kaplan-Meier analysis. (F, G) Gain in OCT1 gene copy number associated with poor survival in both the Singapore cohort (F) and VUMC cohort (G).

performed FISH analysis on six GC tissues and found two samples with gained copy number of OCT1 gene (figure 1F). Combined analysis on the mRNA and CNV data in the TCGA cohort revealed that gained CNV of OCT1 associated with significantly higher mRNA level in GC (figure 1G). In addition, amplifications of OCT1 displayed mutual exclusivity with those of KRAS and FGFR2 genes in the RTK pathway, which are also frequently altered in GC (figure 1H).

OCT1 gene amplification and upregulation associate with poor survival of GC

We further studied the association between OCT1 expression level and different clinicopathological features of GC. When the patients were stratified according to OCT1 expression levels (median split), significantly larger tumour size was found in the OCT1-high group ($p<0.0001$, see online supplementary figure S2A). However, OCT1 was not associated with the sex, age, American Joint Committee on Cancer (AJCC) staging, or any histological subtypes of patients with GC (see online supplementary figure S2B, dataset shown in online supplementary table S1). Notably, OCT1 overexpression strongly associated with poor survival of patients with GC ($p<0.0001$, Mantel-Cox test, figure 2A), and the 5-year survival rate in the OCT1-high group (8.9%) was substantially lower than that of the OCT1-low group (51.1%). In fact, the stratification by OCT1 level displayed even higher prognostic significance than the widely employed AJCC staging (significance $p=0.0002$, 5-year survival: 20 vs 42.2 months, figure 2B). When the GC cases were stratified into four groups according to either OCT1 expression (quartile split) or AJCC staging (I–IV), a better discrimination was also achieved by the OCT1-based method (see online supplementary figure S2C,D). We determined the

receiver operating characteristic curves for the prediction of patient survival using either AJCC stage or OCT1 level, or a combination of both (figure 2C). The area under curve (AUC) of OCT1-based prediction (0.751) was higher than that of the AJCC stage-based model (0.714), while the combination of both factors achieved the highest AUC value (0.800).

Multivariate Cox regression survival analysis adjusting for AJCC stage, tumour size, sex and age of patients consistently reported strong correlation between OCT1 overexpression and shorter survival (p=0.0001, HR=3.27, 95% CI 1.80 to 5.92, figure 2D; also see online supplementary figure S2E). We validated the prognostic significance using the Singapore cohort and found downregulation of OCT1 mRNA significantly associated with survival in patients with GC (p=0.007, Kaplan–Meier analysis, figure 2E).[21] In addition, the gained CNV of OCT1 was also significantly associated with shorter survival, as revealed by the Singapore cohort (p=0.015, figure 2F) and the VUMC GC cohort (p=0.040, figure 2G).[20] These findings consistently suggest OCT1 as a promising prognostic marker for GC cells.

Identification of ERK signalling pathway as regulatory target of OCT1

As described above, the exact pathways that OCT1 may regulate in cancers remain unclear. To probe the OCT1-associated pathways on an unbiased basis, we performed GSEA using high throughput RNA-sequencing data of the GC cohort of The Cancer Genomic Atlas project (TCGA, 282 patients) and a multi-tumour dataset (including 64 human tumours and 27 normal tissue samples) from the Gene Expression Omnibus database.[22] GSEA is designed to detect coordinated differences in expression of predefined sets of functionally related genes.[23] Among all the 189 predefined 'oncogenic signature' gene sets, the PDGF/ERK pathway was identified with the strongest association with OCT1 expression in the TCGA GC dataset (figure 3A) and the multi-tumour dataset (figure 3B). In addition, the Enrichment Map algorithm adjusting for gene set redundancy also identified the RAS-ERK signalling pathway in strong correlation with OCT1 expression (see online supplementary figure S3). Of note, approximately half (2083/4348) of OCT1-correlated genes were found as inducible targets of ELK1,[24] which is a major effector in the ERK signalling pathway (figure 2C). These findings consistently suggest that OCT1 may be involved in the activation of the ERK signalling pathway.

OCT1 expression associates with ERK phosphorylation in GC

In light of the association between OCT1 and ERK signalling, we explored whether OCT1 may correlate with ERK2 expression level or its phosphorylation/activation in GC tissues. Interestingly, analysis on RNA-sequencing data suggested no association between OCT1 and ERK2 mRNA levels (figure 3D), while the tissue immunofluorescence study revealed a strong correlation between OCT1 expression and the level of ERK2 phosphorylation (pERK2) in GC (figure 3E). In addition, the levels of OCT1 and pERK2 were coordinately increased from normal tissues to GC tissues (figure 3F,G). These results suggest potential implication of OCT1 in the phosphorylation/activation of ERK2 in GC.

Regulation of synbindin-mediated ERK phosphorylation by OCT1

Since our group has identified synbindin as a pivotal regulator of ERK2 phosphorylation in GC,[9] we questioned whether OCT1 might affect ERK signalling by regulating synbindin. This assumption was well supported by the putative OCT1-binding sites in the synbindin promoter (within −700 bp upstream of the transcription starting site (TSS); see online supplementary figure S4A). Luciferse reporter assay suggested this promoter region could be transactivated by OCT1 (see online supplementary figure S4B). Further, we performed ChIP assay to test the binding of OCT1 to synbindin promoter in vivo. As a result, the promoter region of synbindin was amplifiable from the DNA recovered from the immunoprecipitation complex using a specific antibody for OCT1 but not a control IgG (see online supplementary figure S4C), thus confirming the binding of OCT1 on the promoter regions of synbindin. To identify the exact binding site of OCT1 on synbindin promoter, we developed a sequence scanning approach using the 3DTF method[25] based on the crystallographic data on the OCT1 protein–DNA complex (pdb entry: 1O4X). The sequence ranging from −253 to −241 upstream of TSS of synbindin was found with the highest binding propensity to OCT1 (figure 4A). To confirm this finding, we analysed the enrichment of OCT1-binding stretches derived from previous ChIP-seq study[26] in the synbindin promoter. This method also identified the −253 to −241 region as the strongest binder to OCT1 (figure 4B). Finally, a luciferase reporter inserted by this short sequence could be strongly transactivated by OCT1 (figure 4C), while other sequences mapping to non-predicted sites were not transactivated (see online supplementary figure S4D,E). These results confirmed the findings of the two dedicated prediction methods, indicating that OCT1 binds to and transactivates −253 to −241 region of the synbindin promoter.

In support of the effect of OCT1 on transactivating synbindin promoter, ectopic expression of OCT1 markedly upregulated synbindin expression at mRNA and protein levels (figure 4D,E). Consistently, inhibition of OCT1 by specific siRNAs significantly decreased mRNA and protein levels of synbindin (figure 4F,G). The expression levels of OCT1 and synbindin showed similar trends in different GC cell lines, which supported the regulatory effect of OCT1 on synbindin (figure 4H,I). Accordingly, the level of phosphorylated ERK (p-ERK) was also higher in the OCT1 and synbindin-expressing cells (figure 4H), although the genetic background of AGS (KRAS mutation) and MKN45 (MET amplification) should also be taken into account. Ectopic expression of OCT1 significantly increased synbindin level and ERK2 phosphorylation in GC cells (figure 4J). The subtle change on total ERK2 level confirmed that OCT1 has little effect on ERK2 expression. Taken together, these results indicate that OCT1 regulates ERK2 phosphorylation/activation by transactivating synbindin in GC cells.

OCT1 as a determinant of synbindin expression in GC tissues

Further, we performed immunofluorescence assay to analyse the expression levels of OCT1 and synbindin in normal gastric mucosa and GC tissues. As shown in figure 5A–C, OCT1 and synbindin protein levels showed remarkable correlation (p<0.0001, Pearson correlation). Consistently, RNA-sequencing data revealed significant correlation between the mRNA levels of OCT1 and synbindin across different cancer types and normal tissues (p<0.0001, Pearson correlation, figure 5D). The relationship between OCT1 and synbindin mRNAs in GC tissues was further analysed using microarray data,[27] which suggested strong correlation between mRNA levels of the two genes (p=0.0002, Pearson correlation, figure 5E). These results, based on human cancer tissues, strongly suggest that OCT1 is a determinant of synbindin expression in GC cells.

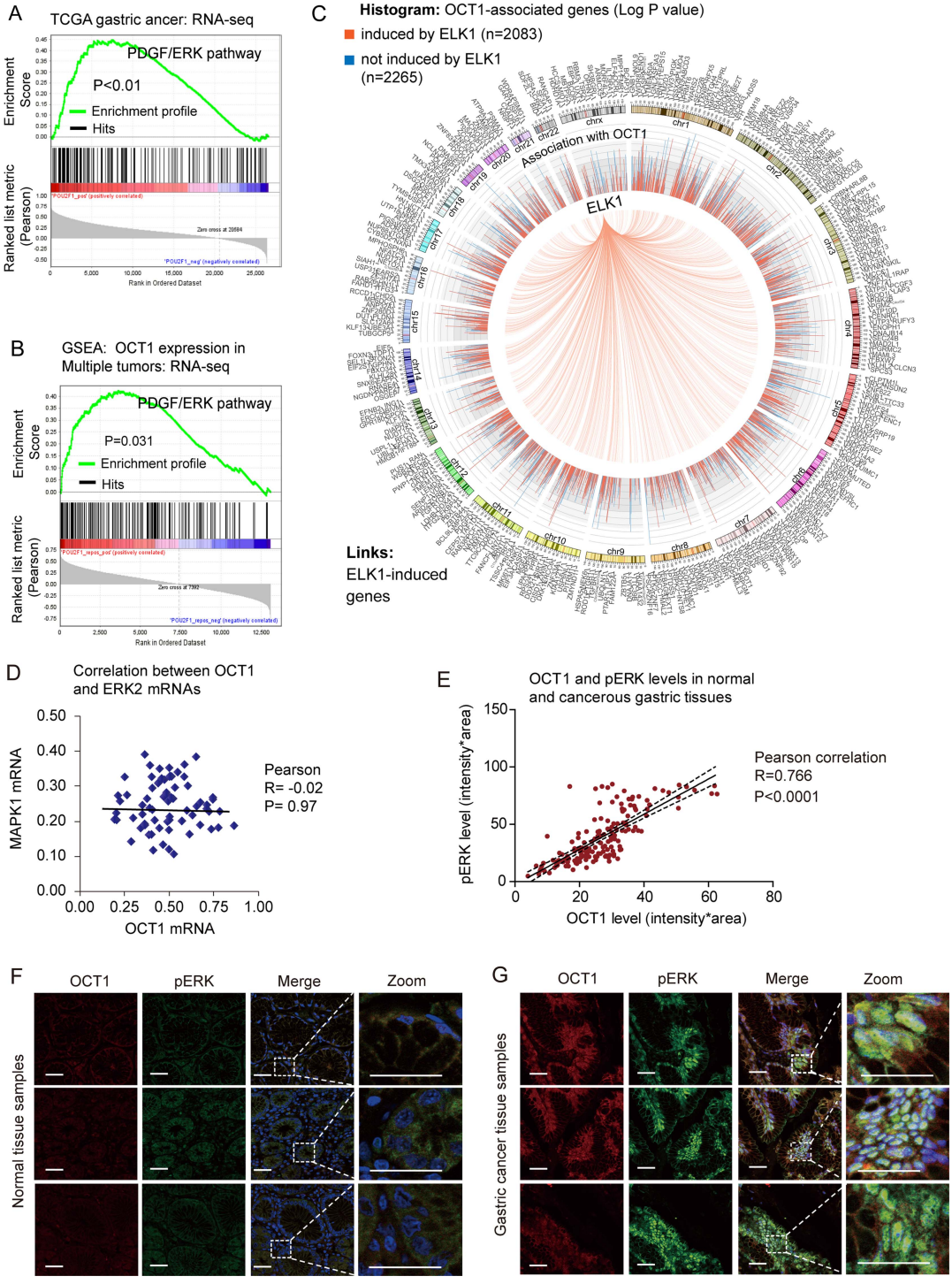

Figure 3 Identification of extracellular signal-regulated kinase (ERK) signalling as a regulatory target of octamer transcription factor 1 (OCT1). (A, B) Gene Set Enrichment Analysis (GSEA) identified significant association between OCT1 and ERK signaling pathway in both the TCGA gastric cancer dataset and the multi-tumor dataset. (C) Circos plot showing 2083 of the 4348 OCT1-associated genes are inducible by ELK1, a major effector gene in ERK signaling pathway. The histogram shows corresponding P values (log1/2 transformed) of the associated genes, with red color representing ELK1-inducible genes while blue indicating non-inducible genes. (D) The expression levels of OCT1 and ERK2 were subjected to Pearson correlation analysis, which suggested no correlation between the two genes (P=0.97). (E) Correlation between the protein levels of OCT1 and phosphorylated ERK (pERK) as determined by immunostain of gastric cancer and normal tissues. (F) Representative immunofluorescent image of OCT1 (labeled in red) and pERK (green) in normal gastric tissues. Zoomed sections are shown on the right panels. Scale bars indicate 100μm in all panels. (G) Representative gastric cancer immunostain images acquired by the same procedures as described previously.

Synbindin-dependent effects of OCT1 in GC cells

To test whether the effects of OCT1 on ERK phosphorylation/activation is dependent on synbindin expression, the human GC MGC803 cells were transfected with OCT1 expression vector or control vector, in the absence or presence of siRNAs specific for synbindin. While OCT1 significantly increased the levels of pERK and pELK1 (without affecting p-MEK level), knockdown of synbindin efficiently suppressed the effects of OCT1 (figure 5F).

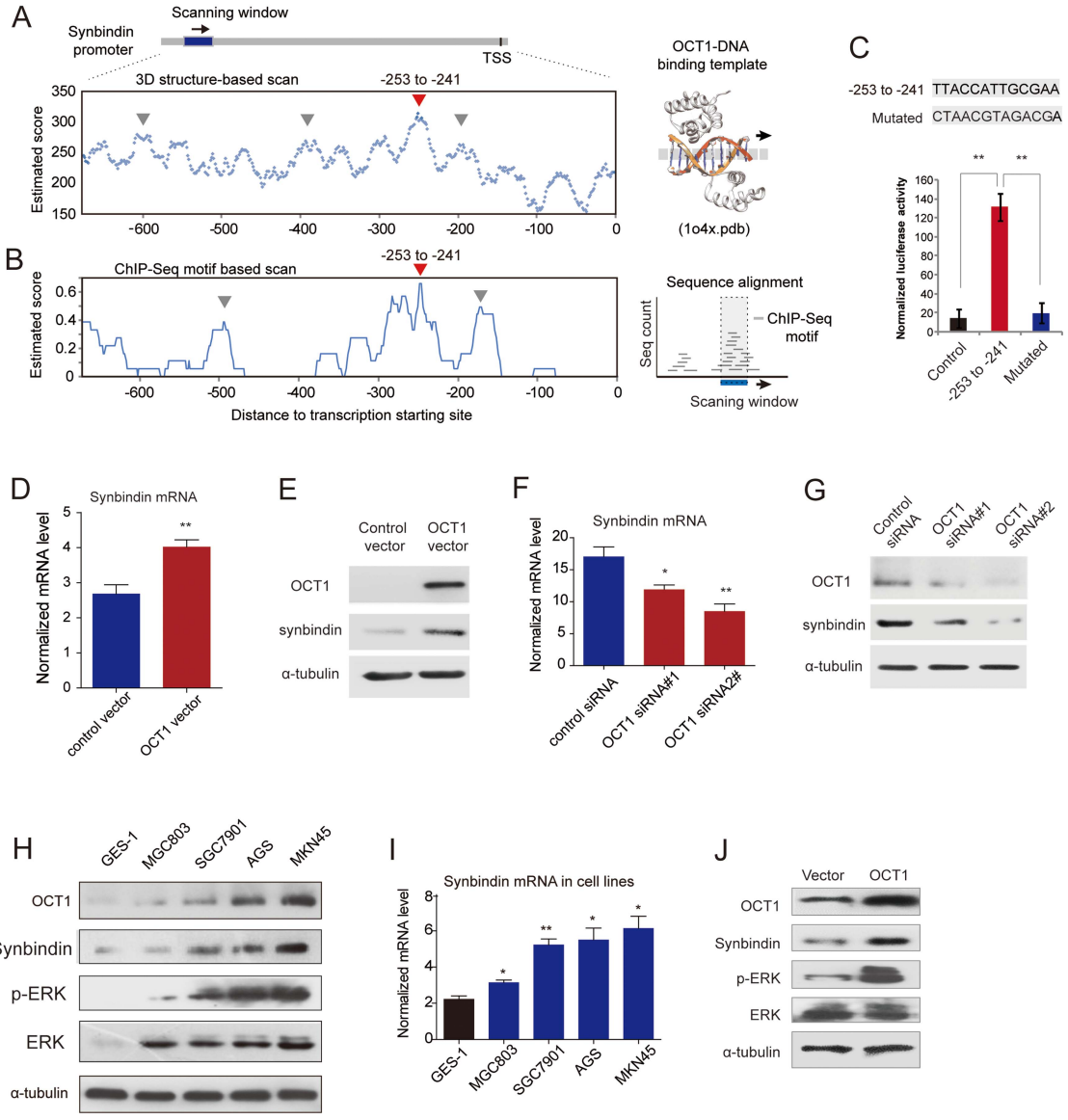

Figure 4 Transactivation of synbindin by octamer transcription factor 1 (OCT1) and effects on extracellular signal-regulated kinase (ERK) activation. (A) TF-DNA crystallography structure-based prediction of OCT1 binding sites on synbindin promoter (OCT1-DNA complex structure shown on the right). Arrow heads in red and in grey respectively indicate the predicted binding sequence and other sequences tested by luciferase assay. (B) ChIP-seq enriched motif-based prediction of OCT1 binding on synbindin promoter (analysis scheme shown in the right panel). (C) The predicted OCT1-binding sequence (-253 to -241) and its mutated variant (both sequences indicated) were respectively inserted into a luciferase reporter and analyzed for their responses to OCT1. (D) Gastric cancer cells were transfected with OCT1 or control vector, and the mRNA level of synbindin was quantified by qPCR. (E) Western Blot of OCT1 and synbindin of cells treated as described as above. (F) Cells were treated by OCT1 siRNAs and control siRNA, and the level of synbindin mRNA was quantified by qPCR. The 18S rRNA level was used for normalization. (G) Western Blot showing decrease of synbindin protein upon knockdown of OCT1 using specific siRNAs. (H) Western blot showing the expression levels of OCT1, synbindin, p-ERK and ERK in five gastric cell lines. OCT1 expression is upregulated in GC cells as compared to normal gastric mucosa cell GES-1. (I) The mRNA level of synbindin in gastric cell lines was detected by RT-qPCR. (J) Cells were transfected by OCT1 or control vector, followed by Western Blot analysis using specific antibodies for synbindin, phosphorylated ERK (pERK) or total ERK.

These results supported our notion that synbindin plays a central role in mediating OCT1-induced ERK signalling.

Moreover, we found that synbindin is required for the effects of OCT1 on the malignant behaviours of GC cells. Transwell assay revealed a significant increase in the invasiveness of OCT1-expressing cells, which could be suppressed by knockdown of synbindin (figure 5F,G). In addition, MTT assay suggested pro-proliferation effect of OCT1 on GC cells (figure 5H), and flow cytometry combined with annexin V-FITC staining indicated the strong anti-apoptotic effect of OCT1 (figure 5I,J). Importantly, suppression of synbindin expression by specific siRNAs impaired these pro-malignant effects of OCT1 (figure 5F–J). Since the MKN45 cells expressed a higher level of OCT1, we examined the effect of suppressing OCT1 on cell proliferation and invasion. As a result, knockdown of OCT1 using specific siRNAs inhibited the proliferation and invasion of MKN45 cells, while ectopic expression of synbindin restored cell proliferation and invasion (figure 5K,L). These results suggest that OCT1 contributes to malignant behaviours of GC cells by regulating synbindin expression.

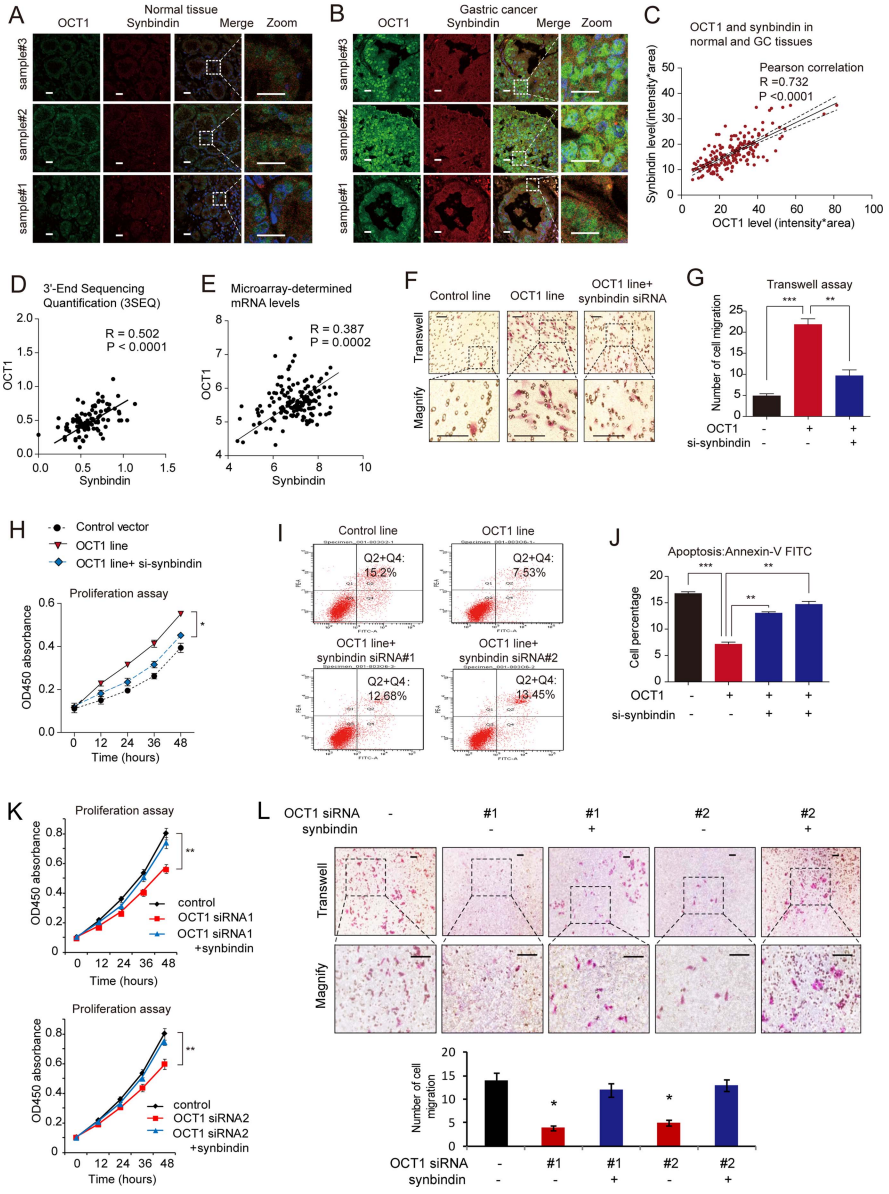

Figure 5 Roles of octamer transcription factor 1 (OCT1) in regulating synbindin expression and cell aggressiveness. (A) Immunofluorescent detection of OCT1 and synbindin expression in normal gastric tissues. Scale bars indicate 20 μm in all panels. (B) Immunostain of OCT1 and synbindin in human gastric cancer tissues. (C) Correlation between the protein levels of OCT1 and synbindin in human gastric cancer tissues as determined by immunofluorescence. (D) The mRNA levels of OCT1 and synbindin determined by RNA-sequencing (GSE28866) showed strong correlation in cancer and normal tissues. (E) The OCT1 and synbindin mRNA levels detected by microarray (GSE27342) were strongly correlated in human gastric tissues. (F) Representative Transwell assays of MGC803 cells stably expressing the control vector or OCT1 vector treated without/with the specific siRNAs for synbindin. Scale bars indicate 100 μm in all panels. (G) Statistical result based on three independent Transwell assays. (H) Cell Counting Kit-8(CCK8) assay of MGC803 cells stably expressing control vector or OCT1 vector without/with treatment by synbindin siRNAs. (I) Apoptosis of cells treated by above-mentioned procedures as measured by flow cytometry combined with phycoerythrin (PE)-conjugated annexin V staining. (J) Statistics based on 3 independent apoptotic assays (**P<0.01; ***P<0.001, t-test). (K) The MKN45 cells were treated by two specific siRNAs (left and right panels) without or with ectopic expression of synbindin, and cell proliferation was measured by CCK8 assay (OD450 absorbance). (L) Effects of OCT1 silencing and synbindin ectopic expression on the invasiveness of MKN45 cells. Scale bars indicate 100 μm in all panels.

OCT1-synbindin signalling promotes ELK1 and RSK phosphorylation

Previous studies suggested that ERK signalling can be spatially separated into substrates that bind to the DEF (docking site for ERK, FXFP) domain or the D (docing) domain.[28] To determine the specific ERK substrates that are affected by OCT1 and synbindin, we used Western blot to detect the phosphorylation of ELK1 (DEF-domain substrate) and RSK (D-domain substrate) in MGC803 cells expressing ectopic OCT1. Interestingly, we found that the phosphorylation of ELK1 and RSK were both increased upon OCT1 upregulation, but the change of p-ELK1 was more pronounced (figure 6A). In support of this, OCT1 silencing in MKN45 cells substantially decreased ELK1 phosphorylation, while synbindin ectopic expression largely restored the p-ELK1 level. In contrast, OCT1 silencing only induced a mild decrease of p-RSK level (see online supplementary figure S5).

Accordingly, knockdown of ELK1 also abrogated the effect of OCT1 overexpression on cell proliferation, but RSK silencing

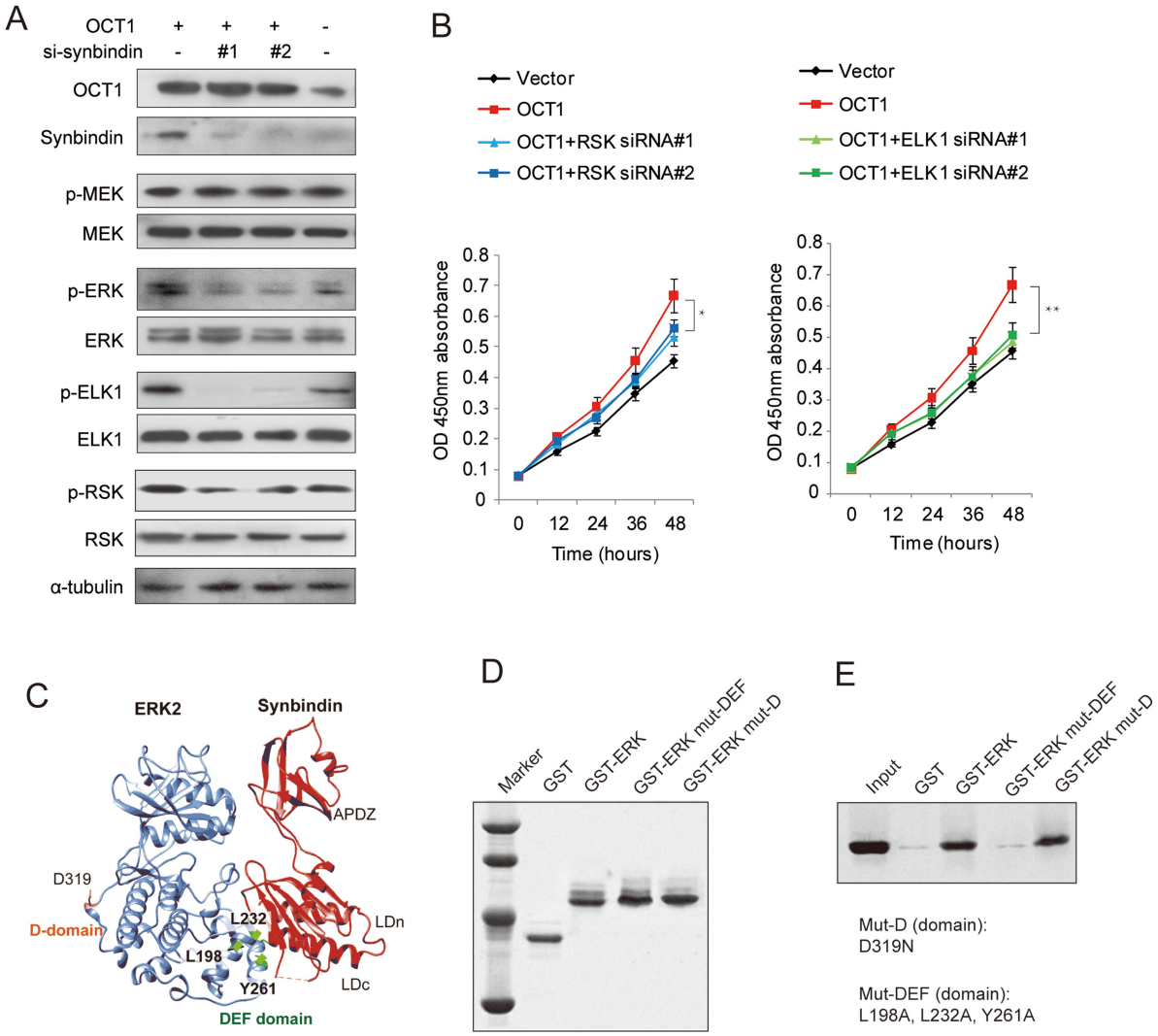

Figure 6 Effects of octamer transcription factor 1 (OCT1) on the phosphorylation of extracellular signal-regulated kinase (ERK) and substrate proteins. (A) Cells were transfected with OCT1 expression vector in the absence or presence of siRNAs specific for synbindin (si-synbindin #1 & #2), and the levels of pERK/ERK, p-ELK1/ELK1, p-RSK/RSK were detected by Western Blot. The α-tubulin level was used as loading control. (B) Effects of ectopic OCT1 expression and knockdown of ERK substrates (RSK and ELK1) on cell proliferation at the last time point (48h) using t-test (*P<0.05, **P<0.01). (C) The Hex spherical polar Fourier protein docking algorithm was employed to probe the synbindin-ERK complex conformation based on the crystallography structures of synbindin (PDB ID code 3EAP) and ERK2 (PDB ID code 2J0Z). (D) Input amount of the ERK mutants in D-domain (mut-D, D319N) and in DEF domain (mut-DEF, L198A, L232A, and Y261A) for GST pull-down assay. (E) The co-immunoprecipitated synbindin protein under each condition is shown in the Western Blot.

only mildly affected the effect of OCT1 (figure 6B). Taken together, our data suggest that ELK1 (docked to DEF domain) plays more important roles in mediating the pro-malignant potentials of OCT1/synbindin.

Mode of synbindin–ERK interaction

We found previously that synbindin binds to MEK and ERK on the Golgi, facilitating ERK phosphorylation by MEK.[9] In addition, the C-terminal Longin (LDc) domain of synbindin was found to interact with ERK protein. Here we further probe the structural motif of ERK that interacts with synbindin by protein–protein docking combined with experimental validation. The Hex spherical polar Fourier protein docking algorithm[29] was implemented to determine the complex conformation of synbindin (PDB ID code 3EAP) and ERK2 (PDB ID code 2J0Z). Intriguingly, the synbindin LDc domain perfectly matched with the ERK DEF domain in terms of geometry and electrostatic complementation (figure 6C). The binding mode resembled the interaction between ERK and PEA-15 (an ERK spatial regulator)[30] and a designed ankyrin repeat protein[31] that has recently been determined by crystallography (see online supplementary figure S6A–C). Since the ERK amino acid residues Leu198, Leu232 and Tyr261 were found to be important for DEF docking,[28] we proposed they might also be involved in the binding to synbindin. To test this, we fused ERK to glutathione S-transferase (GST) and generated mutations to disrupt the above residues (L198A, L232A and Y261A). The GST pull-down assay identified interaction between synbindin and wild-type ERK, which was abolished by mutations in the DEF domain (figure 6D,E). However, the control mutation D319N sitting in the D-domain did not affect the interaction between synbindin and ERK. These data suggest that synbindin binds to the DEF domain of ERK rather than the D domain. Protein docking suggested that synbindin–ERK interaction facilitates subsequent docking of MEK1 to the ERK activation loop (predicted model shown in online supplementary figure S6D),

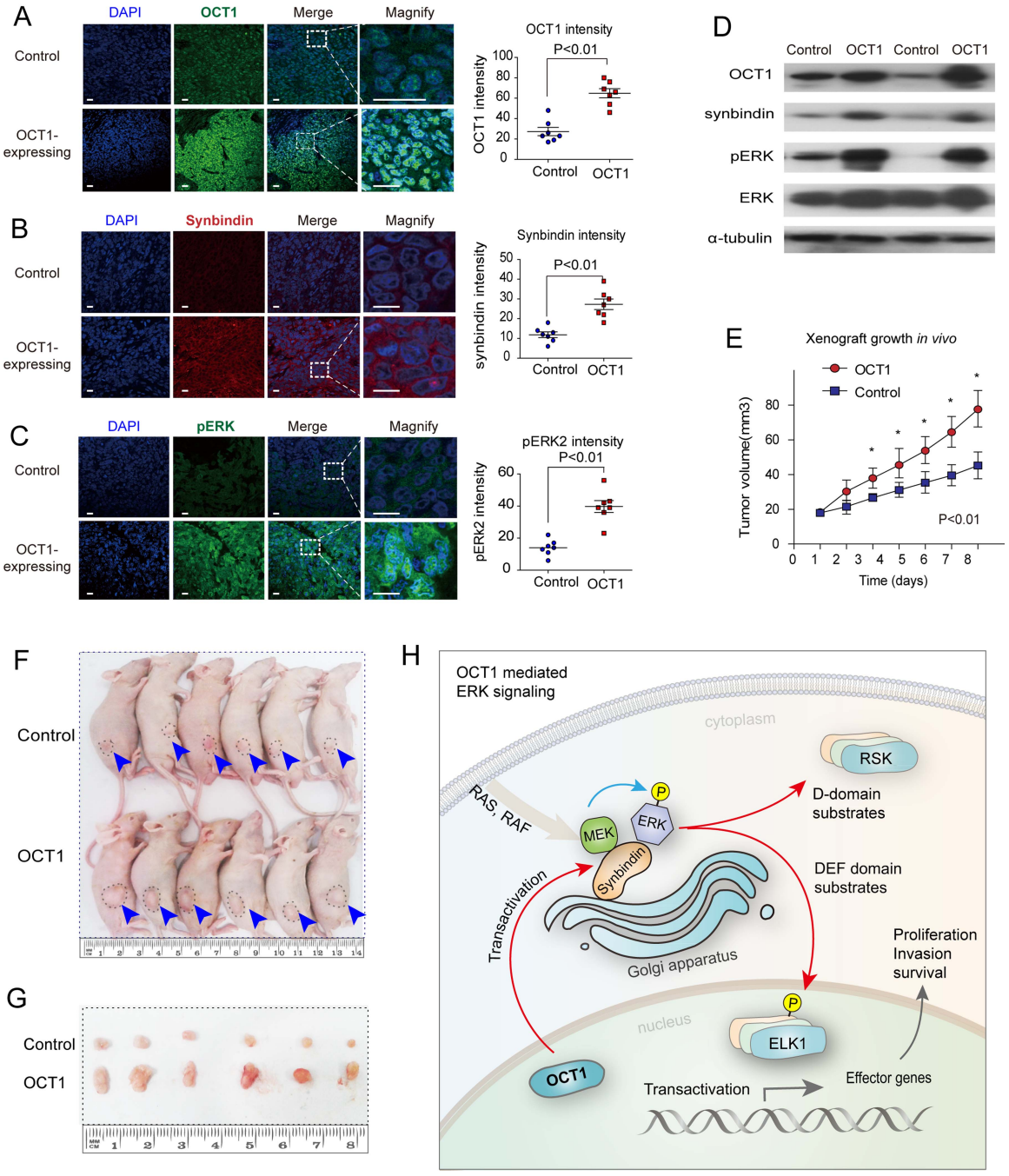

Figure 7 Octamer transcription factor 1 (OCT1) promotes synbindin expression and extracellular signal-regulated kinase (ERK) phosphorylation in vivo. (A) The right panel shows statistical analysis of OCT1 expression based on multiple xenograft tumors (P<0.01, two-sided student t-test). (B) Representative image and statistical analysis of synbindin expression in xenograft tumors expressing OCT1 or control vector. Synbindin is stained using specific antibody in red. Scale bars indicate 10 μm. (C) The level of phoshporylated ERK (pERK) was dramatically increased by the expression of OCT1. (D) Western Blot of xenograft tissues in OCT1-expressing group and control group. (E) Growth curves of xenograft tumors expressing OCT1 or control vector. (F) Nude mice carrying xenograft tumors that expressed OCT1 or control vector. The ranges of tumors are marked by dashed lines. (G) Image of excised tumors expressing OCT1 or control vector. (H) Schematic representation for the OCT1-synbindin-ERK regulatory pathway proposed in this study. OCT1 transactivates synbindin, which is a core subunit of a tether complex on the Golgi involved in vesicle transportation. Synbindin functions as a molecular scaffold that binds to both MEK and ERK2, facilitating ERK phosphorylation on the Golgi apparatus. This promotes the activation of ERK substrates (especially the DEF-domain substrate ELK1), leading to potentiation of cell proliferation and invasion in gastric cancers.

which seems to be relevant to the enhanced activation of ERK observed in our previous study.[9]

Further, we questioned whether potential phosphorylation of synbindin may be involved in this process. By analysing the PhosphoSite database[32] that integrates published phosphorylation data using unbiased high-throughput proteomic approaches, we summarised the frequency of all detected protein phosphorylation in 32 reported GC cell lines (data in online supplementary table S2). The ERK2 protein was found as the most frequently phosphorylated protein in these GC cell lines (see online supplementary figure S6E), which is consistent with a previous report about the high prevalence of

ERK activation in GC.[5] Although 6497 phosphorylation sites were detected in the proteome, no phosphorylation of synbindin was identified in any cell line. Thus, the phosphorylation of synbindin does not seem to be required for ERK activation in GC cells. Taken together, these findings support our notion that synbindin facilitates MEK–ERK interaction and ERK phosphorylation, leading to activation of ERK substrates (proposed model shown in online supplementary figure S6F).

Effects of OCT1 on ERK activation and tumour growth in xenograft mouse model

Finally, we tested whether upregulation of OCT1 could promote tumourigenicity of GC cells in vivo using a xenograft model in nude mice. Stable cell lines carrying either OCT1 expression vector or the control vector were injected subcutaneously to the right flank of nude mice to allow xenograft tumour formation. At 14 days after first injection, mice in the OCT1 group and control group were sacrificed and the xenograft tissues were subjected to Western blot and immunofluorescence analyses. As a result, OCT1 was efficiently upregulated in the OCT1 group compared with the control group (figure 7A). Meanwhile, the expression levels of synbindin (figure 7B) and phosphorylated ERK2 (figure 7C) were significantly higher in the OCT1-upregulated group. These result were also confirmed by Western blot, which revealed a substantial increase in the levels of synbindin and phosphorylated (but not total) ERK2 in the tissues of the OCT1-upregulated group (figure 7D). As a result of enhanced ERK signalling, xenograft tumour growth in the OCT1-upregulated group was significantly faster than that of the control group (figure 7E–G). These results strongly supported our notion that OCT1 promotes gastric carcinogenesis and this effect involves synbindin-mediated ERK signalling activation.

DISCUSSION

The OCT1 transcription factor, a homologue of the OCT4 pluripotency factor, was found to express in GC and its precancerous lesion. However, the functional implication and prognostic value of OCT1 in GC have been poorly defined. In this study we report recurrent amplification and upregulation of the OCT1 gene associated with poor prognosis of patients with GC. In addition, we reveal the underlying mechanism for such an association by demonstrating OCT1 as a determinant of synbindin-mediated ERK signalling and related aggressive phenotypes in GC cells.

First, our study identifies OCT1 as a promising biomarker for the diagnosis and prognosis of GC. OCT1 is significantly upregulated in GC and its precancerous lesion, and the expression of OCT1 can be conveniently detected by histochemistry of tissue biopsy obtained by gastric endoscopy. Thus, OCT1 should be further evaluated for its diagnostic value in early GC. Importantly, the strong association between OCT1 upregulation and poor outcome of patients with GC has been confirmed by our data and an independent dataset. In addition, the prognostic significance of OCT1 CNV is also supported by two independent datasets. These interesting results suggest that OCT1 overexpression (detectable by immunohistochemistry) or gained CNV (by FISH) can be used as prognostic markers in GC. The GSEA indicated that OCT1 overexpression marks activation of the RAS/ERK signalling pathway, thus may provide useful information for targeted therapy.

The recurrent amplification of the OCT1 gene and its prominent ability to increase tumour aggressiveness suggest that OCT1 may play a driving role in gastric carcinogenesis. Thus, targeting OCT1 may present a favourable therapeutic strategy for GC cells, especially for the cases with deregulated ERK signalling. Interestingly, OCT1 has recently been reported to be associated with ERK signalling in oesophageal carcinogenesis,[33] suggesting that OCT1 may affect ERK signalling and cancer aggressiveness in a broader scenario. Thus, it warrants further studies to clarify the clinical and biological relevance of OCT1 in other types of cancers.

By demonstrating the effect of OCT1 on transactivating synbindin, we are able to provide a more complete model for the spatial regulation of ERK signalling on the Golgi apparatus (schematic representation in figure 7H). Apart from the canonical Ras-Raf-MEK-ERK signal transduction flow, recent studies have stressed the importance of ERK signalling regulation in specific subcellular compartments, a so-called 'spatial regulatory' mechanism.[34] In our recent studies,[9] we identified synbindin as a key molecular scaffold that confers spatial regulation of ERK signalling on the Golgi (illustrated in figure 7H). In this study, we further identify OCT1 as an upstream regulator of synbindin in GC and provide structural insight into synbindin-mediated ERK activation. We show that synbindin LDc domain binds to the DEF domain of ERK, leading to phosphorylation of ERK substrates (especially DEF-domain substrate) and increased cell aggressiveness. Importantly, our study on GC tissue samples reported a strong correlation between OCT1 expression and ERK2 phosphorylation levels ($p<0.0001$), suggesting that OCT1 is a crucial regulator for ERK2 activation in GC. The recurrent amplification of the OCT1 gene, together with its regulation on synbindin-related ERK signalling, suggests OCT1 as a potential driver of malignant behaviours of GC cells.

The effects of OCT1 on ERK signalling may also help to explain other reported activities of OCT1. As a homologue of OCT4 pluripotency factor, OCT1 has been found without the ability to induce pluripotency.[35] Instead, OCT1 was suggested to associate with the self-renewal of cancer stem cells[36] and the epithelial–mesenchymal transition (EMT) process.[16] Interestingly, ERK signalling has also been found to be crucial for the stem-like cells in multiple cancers, including GC,[37] colorectal cancer,[38] prostate cancer,[39] breast cancer[40] and glioblastoma.[41] Recent studies have also clearly demonstrated the important roles of ERK signalling in the EMT process.[42–44] Thus, it warrants further study whether OCT1 may contribute to the stem-like behaviours of cancer cells and the EMT process by regulating of the ERK signalling pathway.

In conclusion, our results identify OCT1 as a determinant of synbindin-mediated activation of ERK signalling in GC, and OCT1 is a potential prognostic marker and therapeutic target in GC.

Contributors JQ and JX wrote the paper. JQ, XK, JW, HC and YH conducted the experiments. ND and PT contributed data. JX, HC, WZ and J-YF analysed data. J-YF and JX supervised the research. JQ and XK contributed equally.

Funding This project was supported by grants from the National Basic Research Program of China 973 Program (2010CB5293), the National High Technology Research and Development Program of China 863 Program (2012AA02A504), the Program for Innovative Research Team of Shanghai Municipal Education Commission, and National Natural Science Foundation of China (30971330, 31371420, 81320108024) to JY Fang. The project was also partially supported by National Natural Science Foundation of China (81000861, 81322036, and 81272383), Shanghai 'Oriental Scholars' project (2013XJ), Shanghai Science and Technology Commission 'Pujiang Project' (13PJ1405900), and Shanghai Natural Science Foundation (12ZR1417900) to J Xu. The sponsors of this study had no role in the collection of the data, the analysis and interpretation of the data, the decision to submit the manuscript for publication, or the writing of the manuscript.

Competing interests None.

Patient consent Obtained.

Ethics approval Ethics approval was provided by the Ethics Committee of the Shanghai Jiao-Tong University School of Medicine, Renji Hospital.

Provenance and peer review Not commissioned; externally peer reviewed.

REFERENCES

1 Coupland VH, Lagergren J, Luchtenborg M, *et al*. Hospital volume, proportion resected and mortality from oesophageal and gastric cancer: a population-based study in England, 2004–2008. *Gut* 2013;62:961–6.
2 Camargo MC, Kim WH, Chiaravalli AM, *et al*. Improved survival of gastric cancer with tumour Epstein-Barr virus positivity: an international pooled analysis. *Gut* 2014;63:236–43.
3 Shibata W, Ariyama H, Westphalen CB, *et al*. Stromal cell-derived factor-1 overexpression induces gastric dysplasia through expansion of stromal myofibroblasts and epithelial progenitors. *Gut* 2013;62:192–200.
4 Wang S, Wu X, Zhang J, *et al*. CHIP functions as a novel suppressor of tumour angiogenesis with prognostic significance in human gastric cancer. *Gut* 2013;62:496–508.
5 Paterson AL, Shannon NB, Lao-Sirieix P, *et al*. A systematic approach to therapeutic target selection in oesophago-gastric cancer. *Gut* 2013;62:1415–24.
6 Deng N, Goh LK, Wang H, *et al*. A comprehensive survey of genomic alterations in gastric cancer reveals systematic patterns of molecular exclusivity and co-occurrence among distinct therapeutic targets. *Gut* 2012;61:673–84.
7 Dulak AM, Schumacher SE, van Lieshout J, *et al*. Gastrointestinal adenocarcinomas of the esophagus, stomach, and colon exhibit distinct patterns of genome instability and oncogenesis. *Cancer Res* 2012;72:4383–93.
8 Kholodenko BN, Hancock JF, Kolch W. Signalling ballet in space and time. *Nat Rev Mol Cell Biol* 2010;11:414–26.
9 Kong X, Qian J, Chen LS, *et al*. Synbindin in extracellular signal-regulated protein kinase spatial regulation and gastric cancer aggressiveness. *J Natl Cancer Inst* 2013;105:1738–49.
10 Lee MC, Toh LL, Yaw LP, *et al*. Drosophila octamer elements and Pdm-1 dictate the coordinated transcription of core histone genes. *J Biol Chem* 2010;285:9041–53.
11 Wang VE, Tantin D, Chen J, *et al*. B cell development and immunoglobulin transcription in Oct-1-deficient mice. *Proc Natl Acad Sci U S A* 2004;101:2005–10.
12 Bertolino E, Reddy K, Medina KL, *et al*. Regulation of interleukin 7-dependent immunoglobulin heavy-chain variable gene rearrangements by transcription factor STAT5. *Nat Immunol* 2005;6:836–43.
13 Shakya A, Cooksey R, Cox JE, *et al*. Oct1 loss of function induces a coordinate metabolic shift that opposes tumorigenicity. *Nat Cell Biol* 2009;11:320–7.
14 Jin T, Li H. Pou homeodomain protein OCT1 is implicated in the expression of the caudal-related homeobox gene Cdx-2. *J Biol Chem* 2001;276:14752–8.
15 Almeida R, Almeida J, Shoshkes M, *et al*. OCT-1 is over-expressed in intestinal metaplasia and intestinal gastric carcinomas and binds to, but does not transactivate, CDX2 in gastric cells. *J Pathol* 2005;207:396–401.
16 Hwang-Verslues WW, Chang PH, Jeng YM, *et al*. Loss of corepressor PER2 under hypoxia up-regulates OCT1-mediated EMT gene expression and enhances tumor malignancy. *Proc Natl Acad Sci U S A* 2013;110:12331–6.
17 Ethell IM, Hagihara K, Miura Y, *et al*. Synbindin, a novel syndecan-2-binding protein in neuronal dendritic spines. *J Cell Biol* 2000;151:53–68.
18 Summersgill B, Clark J, Shipley J. Fluorescence and chromogenic in situ hybridization to detect genetic aberrations in formalin-fixed paraffin embedded material, including tissue microarrays. *Nat Protoc* 2008;3:220–34.
19 Goldman M, Craft B, Swatloski T, *et al*. The UCSC cancer genomics browser: update 2013. *Nucleic Acids Res* 2013;41:D949–54.
20 Buffart TE, Carvalho B, van Grieken NC, *et al*. Losses of chromosome 5q and 14q are associated with favorable clinical outcome of patients with gastric cancer. *Oncologist* 2012;17:653–62.
21 Ooi CH, Ivanova T, Wu J, *et al*. Oncogenic pathway combinations predict clinical prognosis in gastric cancer. *PLoS Genet* 2009;5:e1000676.
22 Brunner AL, Beck AH, Edris B, *et al*. Transcriptional profiling of long non-coding RNAs and novel transcribed regions across a diverse panel of archived human cancers. *Genome Biol* 2012;13:R75.
23 Subramanian A, Kuehn H, Gould J, *et al*. GSEA-P: a desktop application for Gene Set Enrichment Analysis. *Bioinformatics* 2007;23:3251–3.
24 Odrowaz Z, Sharrocks AD. ELK1 uses different DNA binding modes to regulate functionally distinct classes of target genes. *PLoS Genet* 2012;8:e1002694.
25 Gabdoulline R, Eckweiler D, Kel A, *et al*. 3DTF: a web server for predicting transcription factor PWMs using 3D structure-based energy calculations. *Nucleic Acids Res* 2012;40:W180–5.
26 Ferraris L, Stewart AP, Kang J, *et al*. Combinatorial binding of transcription factors in the pluripotency control regions of the genome. *Genome Res* 2011;21:1055–64.
27 Cui J, Chen Y, Chou WC, *et al*. An integrated transcriptomic and computational analysis for biomarker identification in gastric cancer. *Nucleic Acids Res* 2011;39:1197–207.
28 Dimitri CA, Dowdle W, MacKeigan JP, *et al*. Spatially separate docking sites on ERK2 regulate distinct signaling events in vivo. *Curr Biol* 2005;15:1319–24.
29 Ritchie DW, Venkatraman V. Ultra-fast FFT protein docking on graphics processors. *Bioinformatics* 2010;26:2398–405.
30 Mace PD, Wallez Y, Egger MF, *et al*. Structure of ERK2 bound to PEA-15 reveals a mechanism for rapid release of activated MAPK. *Nat Commun* 2013;4:1681.
31 Kummer L, Parizek P, Rube P, *et al*. Structural and functional analysis of phosphorylation-specific binders of the kinase ERK from designed ankyrin repeat protein libraries. *Proc Natl Acad Sci USA* 2012;109:E2248–57.
32 Hornbeck PV, Chabra I, Kornhauser JM, *et al*. PhosphoSite: a bioinformatics resource dedicated to physiological protein phosphorylation. *Proteomics* 2004;4:1551–61.
33 Wang Z, Zhu S, Shen M, *et al*. STAT3 is involved in esophageal carcinogenesis through regulation of Oct-1. *Carcinogenesis* 2013;34:678–88.
34 Reiterer V, Fey D, Kolch W, *et al*. Pseudophosphatase STYX modulates cell-fate decisions and cell migration by spatiotemporal regulation of ERK1/2. *Proc Natl Acad Sci U S A* 2013;110:E2934–43.
35 Kang J, Shakya A, Tantin D. Stem cells, stress, metabolism and cancer: a drama in two Octs. *Trends Biochem Sci* 2009;34:491–9.
36 Maddox J, Shakya A, South S, *et al*. Transcription factor Oct1 is a somatic and cancer stem cell determinant. *PLoS Genet* 2012;8:e1003048.
37 Khurana SS, Riehl TE, Moore BD, *et al*. The hyaluronic acid receptor CD44 coordinates normal and metaplastic gastric epithelial progenitor cell proliferation. *J Biol Chem* 2013;288:16085–97.
38 Wang YK, Zhu YL, Qiu FM, *et al*. Activation of Akt and MAPK pathways enhances the tumorigenicity of CD133+ primary colon cancer cells. *Carcinogenesis* 2010;31:1376–80.
39 Rybak AP, Ingram AJ, Tang D. Propagation of human prostate cancer stem-like cells occurs through EGFR-mediated ERK activation. *PloS ONE* 2013;8:e61716.
40 Ahn HJ, Kim G, Park KS. Ell3 stimulates proliferation, drug resistance, and cancer stem cell properties of breast cancer cells via a MEK/ERK-dependent signaling pathway. *Biochem Biophys Res Commun* 2013;437:557–64.
41 Nakada M, Nambu E, Furuyama N, *et al*. Integrin alpha3 is overexpressed in glioma stem-like cells and promotes invasion. *Br J Cancer* 2013;108:2516–24.
42 Zhang W, Mendoza MC, Pei X, *et al*. Down-regulation of CMTM8 induces epithelial-to-mesenchymal transition-like changes via c-MET/extracellular signal-regulated kinase (ERK) signaling. *J Biol Chem* 2012;287:11850–8.
43 Ha GH, Park JS, Breuer EK. TACC3 promotes epithelial-mesenchymal transition (EMT) through the activation of PI3 K/Akt and ERK signaling pathways. *Cancer Lett* 2013;332:63–73.
44 Elsum IA, Martin C, Humbert PO. Scribble regulates an EMT polarity pathway through modulation of MAPK-ERK signaling to mediate junction formation. *J Cell Sci* 2013;126:3990–9.

SUPPLEMENTAL INFORMATION

Supplemental Methods

Chromatin-immunoprecipitation (ChIP)

ChIP was performed in a similar process as previously reported . Briefly, cells were fixed with 0.5% formaldehyde for 10 minutes at room temperature and subsequently treated with 125 mmol/L glycine for 10 minutes. For each ChIP assay 1x107 Cells were lysed in 750µL lysis buffer [10 mmol/L Tris-Cl (pH8.0), 10 mmol/L EDTA, 0.5 mmol/L EGTA, 0.25% Triton X-100, protease inhibitor cocktail]. Lysates were incubated for 15 minutes at room temperature with rotation and centrifuged. The pellet was resuspended in enrichment buffer [10 mmol/L Tris-Cl (pH 8.0), 200 mmol/L NaCl, 10 mmol/L EDTA, 0.5mmol/L EGTA, protease inhibitor cocktail]. The preparation was incubated for an additional 15 minutes at room temperature with rotation. Insoluble material was pelleted, resuspended in 1 mL immunoprecipitation buffer [20 mmol/L Tris-Cl (pH 8.0), 200 mmol/L NaCl, 0.5% Triton X-100, 0.05%sodium deoxycholate, 0.5% NP40, protease inhibitor cocktail], and sonicated to generate fragmented chromatin with approximately 500 bp in length. For each ChIP, 1µg antibody for OCT1, or 1µg nonspecific immunoglobulin G (Sigma) was added and incubated overnight at 4°C. Immune complexes were precipitated for 1 hour at room temperature with 1/20th volume protein-G beads. Beads were washed three times with immunoprecipitation buffer, once with high salt buffer (immunoprecipitation buffer with 800 mmol/L NaCl), once in LiCl buffer [10 mmol/L Tris-Cl (pH 8.0), 250 mmol/L LiCl, 1% Triton X-100, 0.5% NP40, 0.1% sodium deoxycholate, 5 mmol/L EDTA, protease inhibitor cocktail], and twice with Tris-EDTA. Immune complexes were eluted with 40 µL elution buffer [10 mmol/L Tris-Cl (pH8.0), 1% SDS, 5 mmol/L EDTA] at 65°C for 1 hour and cross-links were reversed by adding 200 mmol/L NaCl and incubating at 65°C overnight. Eluted material was treated with 30 µg proteinase K for 2 hours at 42°C and purified (QIAGEN). Amplification of DNA from OCT1 ChIP was carried out with PCR reaction containing 12.5µL SYBR green master mix (QIAGEN), 7µL water, 3µL of 5µM primer mix, and 2.5µL

DNA. An iCycler iQ real-time PCR detection system (Bio-Rad) was used to perform the quantitative PCR.

Cell viability assays

The MGC803 cells transfected with OCT1 vector in the presence or absence of synbindin siRNA and control vector were seeded onto 96-well plates at 2500cells/well. Cell proliferation was measured using the Cell Counting Kit-8 (CCK-8, Dojindo). At each time point, cells were incubated with 10mL CCK-8 reagent per well (100 ml medium/well) for 30min at 37°C, 5% CO_2. The absorbance was measured at 450 nm.

Flow cytometric analysis

Cell cycle progression was assayed by DNA content using propidium iodide and flow cytometry. MGC803 cells were transfected with OCT1 vector, OCT1 vector+synbindin siRNA and control vector. Approximately 1×106 cells were trypsinized and washed twice with ice-cold PBS and then fixed overnight at -20°C in 70% ethanol. Immediately before flow cytometry, the cells were resuspended in PBS containing propidium iodide (50 μg/ml) and DNase-free RNase (10 μg/ml). Flow cytometry was performed using a FACScalibur (BD biosciences) system with CELLquest software.

Tumor cell invasion assays

Tumor cell invasion assays were performed using Boyden chambers with filter inserts (pore size, 8-μm) coated with Matrigel (40 μg; Collaborative Biomedical, Becton Dickinson Labware, Bedford, MA) in 24-well dishes (Nucleopore, Pleasanton, CA, USA) as described previously [1]. Briefly, 1×10^5 cells after transfected with OCT1 vector in the presence or absence of synbindin siRNA were seeded in the upper chamber, while the same medium was placed in the lower chamber. The plates were incubated for 24 h. Then the cells were fixed in 4% formaldehyde and stained with 0.05% crystal violet in PBS for 20min at room temperature. Cells on the upper side of the filters were removed by cotton-tipped swabs, and the filters were washed with PBS. The cells on the lower side of the filters were defined as invasive cells and counted at x200 magnification in 10 different fields of each filter.

Annexin V analysis

The apoptotic status was analyzed by using a TACS annexin V-FITC kit (R&D Systems, Minneapolis, MN). Briefly, cells (1×10^6cells/mL) were transfected with OCT1 vector in the presence or absence of synbindin siRNA. After washing in ice-cold PBS, cells were collected by EDTA treatment and incubated with a mixture of annexin V-FITC and PI for 15 minutes at room temperature according to the manufacturer's instruction. Early apoptotic (only annexin V-positive) cells were distinguished from late apoptotic or necrotic (annexin V and PI double-positive) cells by a flow cytometric analysis.

Array-based Copy Number Variation (CNV) analysis

The altered chromosome segments in 293 stomach adenocarcinoma patients of The Cancer Genome Atlas (TCGA) cohort were obtained via the UCSC cancer genome browser [2], and the CNV data of Singapore cohort can be accessed from GEO database (GSE31168). Both datasets were based on the Affymetrix SNP6.0 microarray, and were analyzed by GISTIC 2.0 algorithm [3] using default parameters for 'threshold' and 'focal' modes, respectively. The VUMC data were based on customized array-CGH method, and was obtained from GEO database (GSE26389). The compatible CGHCall algorithm [4] was used calculate the CNV of all genes for in VUMC dataset. To identify significant relationships between the CNVs of OCT1 and other genes, a dimension reduction permutation (DRP) statistical algorithm was used to analyze the TCGA CNV dataset. The DRP algorithm has been described previously [5].

Gene Set Enrichment Analysis (GSEA)

GSEA is a method of analyzing and interpreting microarray and such data using biological knowledge [6]. The data in question is analyzed in terms of their differential enrichment in a predefined biological set of genes (representing pathways). These predefined biological sets can be published information about biochemical pathway or coexpression in a previous experiment. GSEA was performed using GSEA version 2.0 from the Broad Institute at MIT. Two datasets were analyzed by GSEA: a 'multi-cancer' dataset [7] including 64 solid tumors and 27 normal tissues (GSE28866) and The Cancer Genome Atlas (TCGA) dataset including 282 GC samples. Both datasets were determined by 3'-End Sequencing for Expression Quantification (3SEQ). In this study, GSEA firstly

generated an ordered list of all genes according to their correlation with OCT1 expression, and then a predefined gene set (signature of gene expression upon perturbation of certain cancer-related gene) receives an enrichment score (ES), which is a measure of statistical evidence rejecting the null hypothesis that its members are randomly distributed in the ordered list. Parameters used for the analysis were as follows. The "c6.all.v4.0.symbols.gmt" gene sets were used for running GSEA and 1000 permutations were used to calculate *P*-value and permutation type was set to gene_set. The maximum gene set size was fixed at 1500 genes, and the minimum size fixed at 15 genes. The expression level of OCT1 (POU2F1) was used as phenotype label, and "Metric for ranking genes" was set to Pearson Correlation. All other basic and advanced fields were set to default.

To overcome gene-set redundancy and help in the interpretation of altered pathways, we applied the "Enrichment Map" algorithm, a network-based method for interpreting gene-set enrichment results [8]. Gene-sets are organized in a network, where each set is a node and links represent gene overlap between sets. Automated network layout groups related gene-sets into network clusters, helping to identify the major enriched functional themes. The default parameters were used to generate enrichment networks: P-value cutoff=0.005; FDR Q-value cutoff=0.1; overlap coefficient cutoff=0.75.

Prediction of OCT1 binding sites by 3D structure-based energy calculations

An initial assignment using the TFsearch prediction tool indicated potential OCT1-binding sites within the synbindin promoter (ranged from -700 to TSS). Then, a more dedicated 3D structure-based method was used to identify OCT1-binding site with higher confidence.

Prediction of OCT1 binding sites based on ChIP-seq data

The features of OCT1- binding sequences can be interpreted by the enriched stretches in OCT1 ChIP-seq data. A previous study has identified 5-mer stretches that are specifically enriched in top 1% OCT1-binding sequences [9]. We analyzed the enrichment of OCT1-binding motifs within the scanning window (described above) as a measure to

search for potential OCT1 binding site in the synbindin promoter. This method was combined with 3DTF algorithm to identify highly confident candidate sequences.

Western blotting

Western blot assays were performed to examine OCT1 and synbindin proteins. Cell extracts were prepared using RIPA buffer (Thermo Fisher) from cells that were treated as indicated. After electrophoresis, proteins were electroeluted at 120 volts onto a polyvinylidene difluoride (PVDF) membrane (Invitrogen). Primary antibodies raised OCT1 were purchased from Abcam. The anti-synbindin antibody was purchased from Abnova, and the α-tubulin antibody was used as a control. The Western blotting analysis was repeated at least three times.

***In vivo* experiments**

Briefly, male BALB/c athymic nude mice (4–6 weeks old) were obtained from the experimental animal center of Shanghai Institute for Biological Sciences (SIBS). All mice were injected subcutaneously into the right side of back with 1.0×107 stable MGC803 cells transfected with OCT1 vector and control vector to establish the GC xenograft model. 14 days after first injection,the two groups were sacrificed and the xenograft tissues were taken for Western blot and Immunofluorescence. Tumor diameters were measured at regular intervals with digital calipers, and tumor volume was calculated by the formula: tumor volume (mm3) = shorter diameter2 × longer diameter/2. The tumor volume data are presented as means ± SD (n = 6).

Supplementary Figures

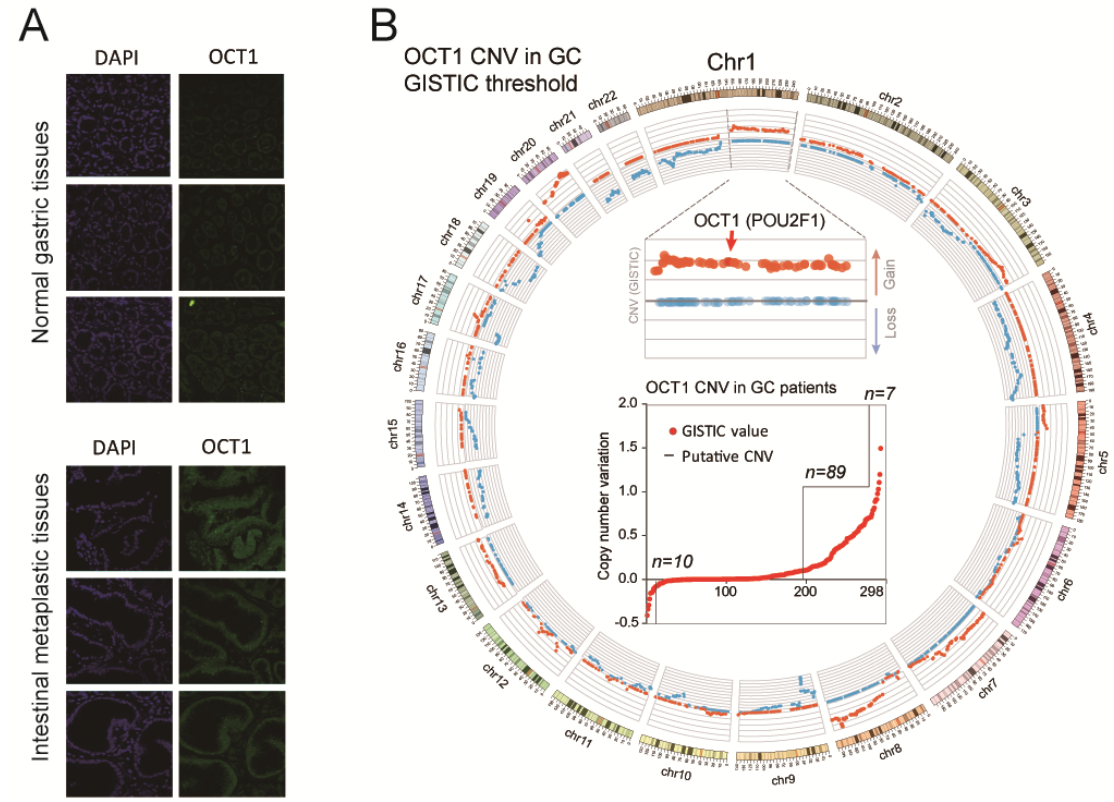

E

Dataset	OCT1 CNV in GC patients			Estimation algorithm
	Gain	All	% with gain	
TCGA cohort	31	305	10.16	GISTIC focal
	98	305	32.13	GISTIC threshold
Singapore cohort	18	193	9.33	GISTIC focal
	54	193	27.98	GISTIC threshold
VUMC cohort	40	180	22.22	CGHCall

Figure S1. Expression and amplification of OCT1 gene in gastric tissues.

(**A**) OCT1 is upregulated in intestinal metaplastic tissues. The upper panel shows OCT1 immunofluorescent staining (green) in normal gastric tissue, while the lower panel presents OCT1 expression in intestinal metaplastic tissues. Cell nucleus were stained with DAPI in blue.

(**B**) The Circos plot shows gene copy number variation (CNV) in the TCGA stomach adenocarcinoma (STAD) cohort. The level of CNV was based on the mean aggregation of log ratio signals of all probes within each gene, regardless of the level of alterations (focal or broad). OCT1 is located in a recurrently amplified region in chromosome 1 (magnified plot). The lower plot shows the CNV (log2 ratio and GISTIC-estimated events) of OCT1 in all patients by increasing order. While the copy number of OCT1 was increased in 96 cases, it was decreased in only 10 patients.

(**C**) Heat map showing CNVs of the TCGA gastric cancer cohort including both broad and focal events. Each column represents a segmented genomic region, and each row represents a GC patient.

(**D**) Focal CNV events in TCGA gastric cancer cohort, wherein the broad CNV events have been subtracted.

(**E**) Summary on the prevalence of OCT1 amplification in three indicated GC cohorts. The TCGA and Singapore datasets (based on SNP array platform) were analyzed by GISTIC algorithm for focal and broad CNV events. The frequencies for OCT1 amplification (including both focal and broad events) were respectively 32.1% (TCGA cohort) and 28.0% (Singapore cohort). Focal amplification of OCT1 was found in 10.2% cases in TCGA cohort and 9.3% patients in Singapore cohort. The VUMC dataset was based on ArrayCGH platform and analyzed CGHCall algorithm, which revealed 22.2% GC cases with amplified OCT1 gene.

A

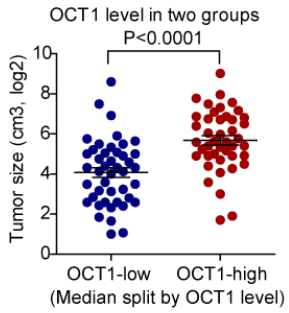

B

Clinical features	OCT1-low	OCT1-high	Significance (P-value)
Total number	45	45	-
Sex (male)	37	30	0.5237 (Chi-square)
Age (years)	65.3	65.7	0.6194 (Mann-Whitney)
Tumor size (cm3)	34.5	82.9	**<0.0001** (Mann-Whitney)
AJCC stage I	5	1	0.3686 (Chi-square)
AJCC stage II	14	16	
AJCC stage III	25	26	
AJCC stage IV	1	2	

C

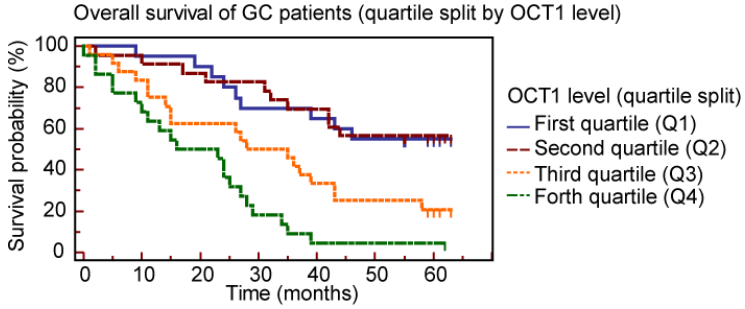

Number at risk

Q1	20	19	18	14	13	11	4
Q2	23	21	20	19	16	13	8
Q3	24	20	15	12	8	6	2
Q4	21	15	11	4	1	1	1

P =0.925 (Q1 vs Q2)

P =0.010 (Q2 vs Q3)

P =2.1x10^{5} (Q3 vs Q4)

D

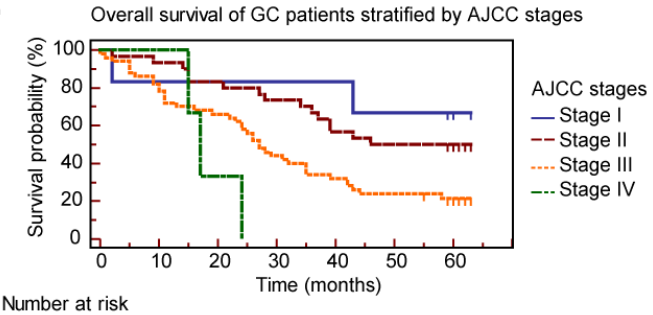

Number at risk

Stage I	6	5	5	5	5	4	1
Stage II	30	28	25	22	17	15	8
Stage III	49	39	33	22	16	12	6
Stage IV	3	3	1	0	0	0	0

P=0.481 (I vs II)

P=0.006 (II vs III)

P=0.136 (III vs IV)

E

Factors	P-value	Exp (b)	95% CI of Exp (b)
OCT1 level	0.0001	3.2658	1.8004 to 5.9239
AJCC stage	0.0068	1.9438	1.2046 to 3.1366
Tumor size	0.1081	1.6526	0.8983 to 3.0403
Sex (female)	0.8658	0.9494	0.5214 to 1.7287
Age	0.0475	1.0253	1.0004 to 1.0508

Figure S2. Association between OCT1 expression and clinicopathological patterns of GC.

(**A**) Statistical analysis on the staining intensity of OCT1 in patients stratified by tumor

sizes (median split). Tumors with larger sizes showed significantly higher OCT1 staining intensity than those with smaller tumor sizes ($P<0.0001$, Mann Whitney test).

(**B**) Association between OCT1 expression and clinicopathological features of gastric cancer patients. All 90 patients were stratified by OCT1 expression levelinto OCT1-low and OCT1-high groups (median split), and the clinicopathological features were compared between two groups using the statistical method indicated.

(**C**) Gastric cancer patients (n=90) were divided into 4 groups according to OCT1 expression levels (quartile split into Q1-Q4), and their survival were compared using Kaplan-Meier survival analysis. The numbers of cases at risk are shown in the lower panel. Significant differences were found between the pairs Q1 v.s. Q3 ($P=0.017$), Q2 v.s. Q3 ($P=0.010$), and Q3 v.s. Q4 ($P=2.1x10^{-5}$).

(**D**) Survival of patients with different AJCC grades were compared by Kaplan-Meier survival analysis. Significant different was only found between the groups with AJCC state II and stage III ($P=0.006$).

(**E**) Multivariate Cox regression survival analysis suggested independent prognostic value of OCT1. Different factors (including OCT1, AJCC stage, tumor size, sex and age) were analyzed for their association with patient survival using Cox regression model. The *P*-value, Exp (b) (hazard ratio) and its 95% confident interval (CI) are shown for each factor.

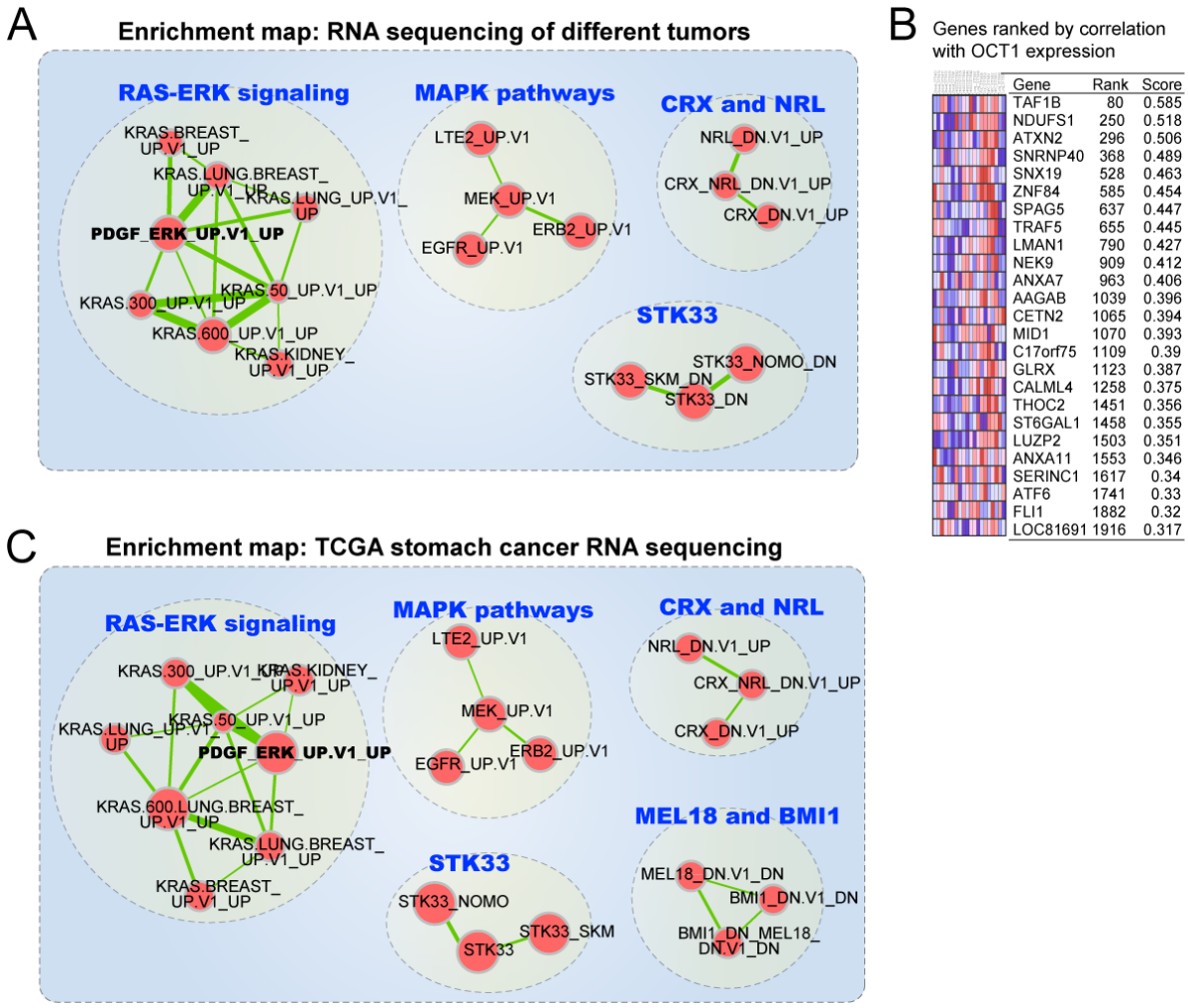

Figure S3. Enrichment map summary of GSEA on OCT1-associated pathways .

(**A**) OCT1-associated gene sets were identified by GSEA on gene expression profiles in multiple tumors. The multi-cancer dataset (GSE28866) included 64 solid tumors and 27 normal tissues, and a ranked gene list was calculated according to the correlation with OCT1 expression. Detailed analysis method for can be found in Methods section. The Enrichment Map analysis was used to overcome gene-set redundancy and improve the interpretation of large gene lists. Multiple gene sets related to RAS-ERK signaling were found to be associated with OCT1 expression (dashed circle), with PDGF/ERK signature as the most correlated gene set. Other clusters of gene sets include MAPK pathways, CRX and NRL, STK33, etc.

(**B**) The expression of ranked genes in the PDGF/ERK signature is shown in the heat map.

(**C**) The OCT1-associated gene sets were determined using TCGA stomach adenocarcinoma (STAD) gene expression profiles. The expression of all genes were determined by 3' RNA sequencing method, and the GSEA/Enrichment Map analyses were performed using the same approaches as in (**A**). The TCGA gastric cancer data also identified the strong correlation between OCT1 expression and RAS-ERK signaling, with PDGF/ERK signature being the most correlated gene set.

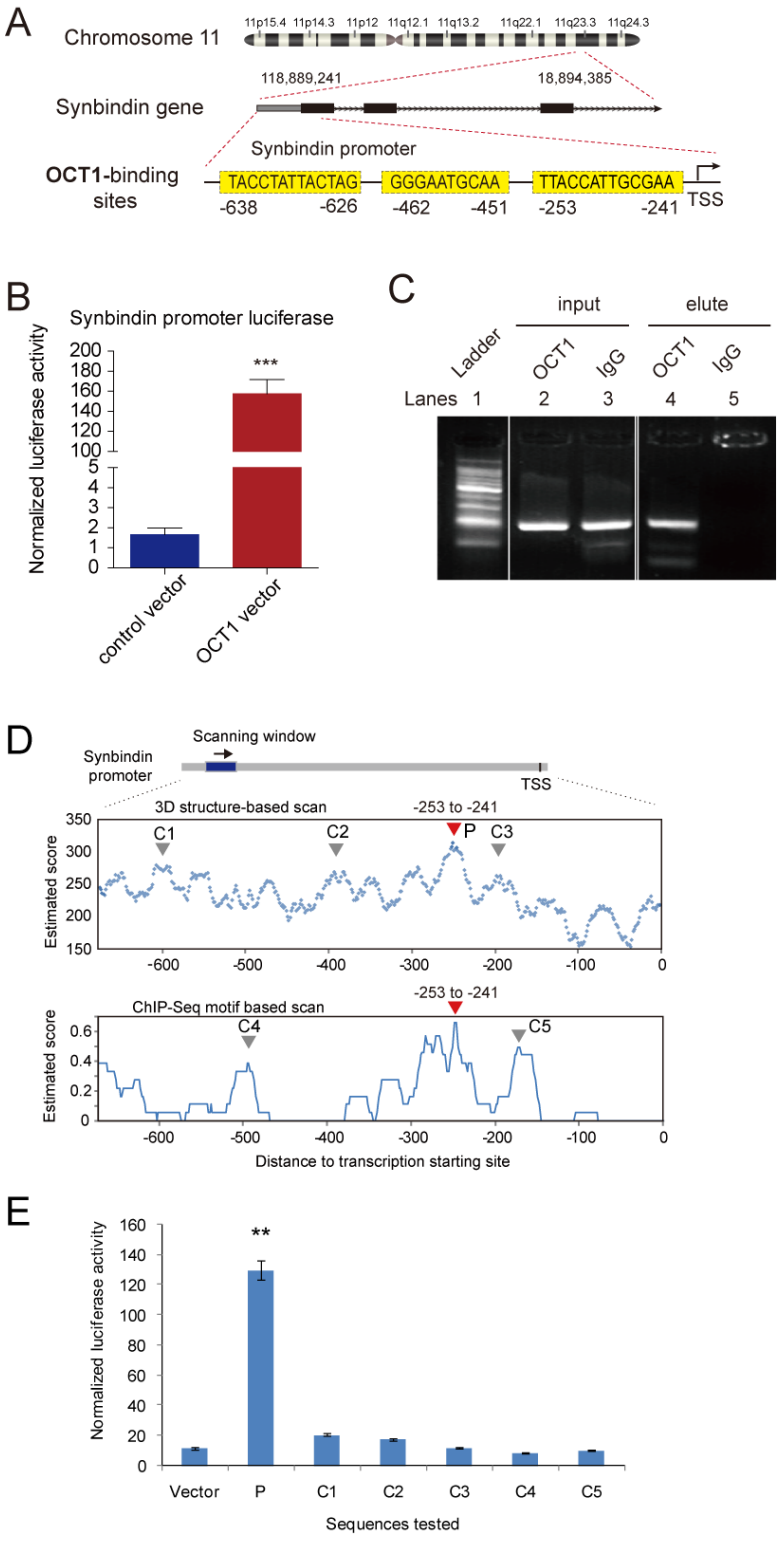

Figure S4. OCT1 binds to the promoter region of synbindin.

(**A**) An initial assignment on OCT1-binding sites on the synbindin promoter using the TFsearch prediction tool. The putative OCT1-binding sites were found upstream (-700) of the transcription start site (TSS) of synbindin gene.

(**B**) Luciferase reporter assay showing the transactivation of synbindin promoter by

OCT1. The synbindin promoter sequence (-654 to -241bp upstream of TSS) was inserted to a reporter vector, and then co-transfected with OCT1 in MGC803 cells. Ectopic expression of OCT1 strongly increased luciferase activity (*** $P<0.001$, two-sided student t-test).

(**C**) Chromatin immunoprecipitation (ChIP) assay showing the binding of OCT to synbindin promoter *in vivo*. The promoter region of synbindin was amplified from the DNA recovered from the immunoprecipitation complex using a specific antibody for OCT1. The input DNA and ChIP yield using non-specific IgG are included as controls.

(**D**) The sequences tested in luciferase assays were picked up from the prediction results by 3DTF (upper panel) and ChIP seq-based (lower panel) methods. The red arrow heads show the position of the true binding site, while grey arrow heads indicate the other tested sequences.

(**E**) Luciferase assay revealed that OCT1 transactivates the predicted binding site (marked as 'P') but not other control sites (C1-C5). (** $P<0.01$, t-test)

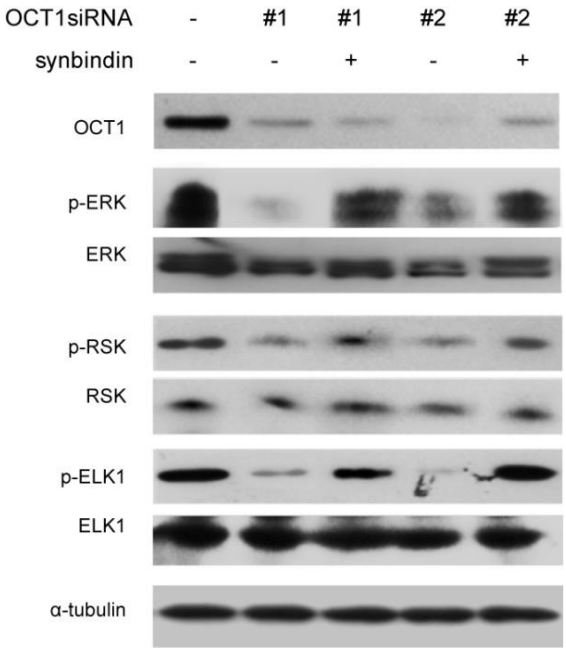

Figure S5. Effects of OCT1 silencing and synbindin ectopic expression on the phosphorylation of ERK and substrates in MKN45 cells.

The MKN45 cells were transfected with siRNAs for OCT1 (#1 and #2, respectively) in the absence or presence of synbindin expression vector, and Western Blot was used to determined the levels of the indicated proteins/phosphor-proteins. While OCT1 silencing suppressed phosphorylation of ERK/RSK/ELK1, synbindin overexpression blocked the effect of OCT1 silencing.

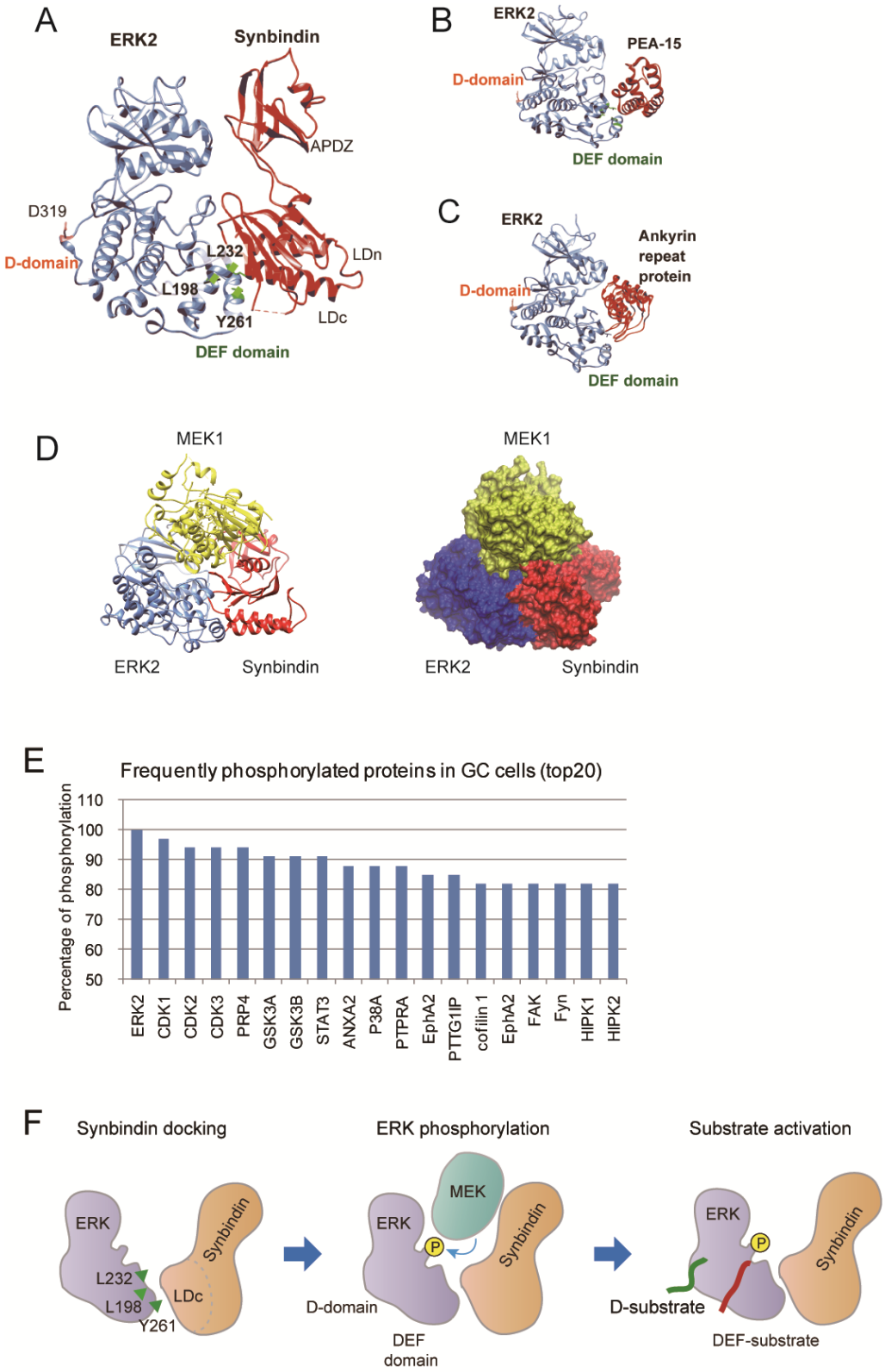

Figure S6. Synbindin binds to DEF-domain of ERK2 protein

(**A**) The binding mode of ERK-synbindin complex as predicted by the Hex spherical polar Fourier protein docking algorithm. In this model, the LDc domain of synbindin interacts with the DEF-domain of ERK2, in contact with its residues L191, L232 and Y261.

(**B**) Crystallography-determined structure of ERK/PEA15 binding complex (PDB accession 4IZA), wherein PEA15 binds to the DEF-domain of ERK but not D-domain.
(**C**) The structure of ERK binding to a designed Ankyrin Repeat protein, based on crystallography data (PDB accession 3ZUV). The DEF-domain of ERK is also involved in the interaction with Ankyrin Repeat protein.
(**D**) The ERK2/synbindin heteroduplex structure (validated by GST pull-down) created a binding surface to MEK1, and the picture shows a predicted structure of MEK1 binding to the ERK2/synbindin duplex. These results suggest that synbindin may facilitate MEK1/ERK2 interaction.
(**E**) The histogram shows the most frequently phosphorylated proteins found in gastric cancer cell lines, based on the PhosphoSite database (combined data from high-throughput proteomic experiments). The phosphorylation of ERK2 protein was identified in all the 32 analyzed gastric cancer cell lines, which represents the most frequent phosphorylation event in the whole proteome. Altogether 6496 proteins were found phosphorylated by different frequencies, ranging from 1/32 to 32/32. Synbindin was not found phosphorylated in any analyzed cell line, suggesting its phosphorylation is not required for ERK phosphorylation in GC cells.
(**F**) Proposed model for synbindin-involved ERK activation. The left panel shows the interaction between synbindin LDc domain and ERK DEF-domain (experimentally validated), which creates a binding surface for MEK1. The binding with MEK1 facilitates ERK phosphorylation (middle panel), which enables ERK to activate its substrates docked to DEF and D-domains (right panel).

Supplemental References

1 Kong X, Qian J, Chen LS, Wang YC, Wang JL, Chen H*, et al.* Synbindin in extracellular signal-regulated protein kinase spatial regulation and gastric cancer aggressiveness. Journal of the National Cancer Institute 2013;**105**:1738-49.

2 Goldman M, Craft B, Swatloski T, Ellrott K, Cline M, Diekhans M*, et al.* The UCSC Cancer Genomics Browser: update 2013. Nucleic acids research 2013;**41**:D949-54.

3 Mermel CH, Schumacher SE, Hill B, Meyerson ML, Beroukhim R, Getz G. GISTIC2.0 facilitates sensitive and confident localization of the targets of focal somatic copy-number alteration in human cancers. Genome biology 2011;**12**:R41.

4 van de Wiel MA, Kim KI, Vosse SJ, van Wieringen WN, Wilting SM, Ylstra B. CGHcall: calling aberrations for array CGH tumor profiles. Bioinformatics 2007;**23**:892-4.

5 Ding L, Getz G, Wheeler DA, Mardis ER, McLellan MD, Cibulskis K*, et al.* Somatic mutations affect key pathways in lung adenocarcinoma. Nature 2008;**455**:1069-75.

6 Subramanian A, Kuehn H, Gould J, Tamayo P, Mesirov JP. GSEA-P: a desktop application for Gene Set Enrichment Analysis. Bioinformatics 2007;**23**:3251-3.

7 Brunner AL, Beck AH, Edris B, Sweeney RT, Zhu SX, Li R*, et al.* Transcriptional profiling of long non-coding RNAs and novel transcribed regions across a diverse panel of archived human cancers. Genome biology 2012;**13**:R75.

8 Merico D, Isserlin R, Stueker O, Emili A, Bader GD. Enrichment map: a network-based method for gene-set enrichment visualization and interpretation. PloS one 2010;**5**:e13984.

9 Ferraris L, Stewart AP, Kang J, DeSimone AM, Gemberling M, Tantin D*, et al.* Combinatorial binding of transcription factors in the pluripotency control regions of the genome. Genome research 2011;**21**:1055-64.

Supplementary Table 1. OCT1 expression levels and clinical features of gastric cancer cases.

Survival time (months)	Survival status	Tumor size (cm3)	Sex	Age (years)	AJCC stages	OCT1 level
59	Alive	3.15	Male	72	II	11.213
59	Alive	8.75	Male	49	I	15.429
55	Alive	60	Male	52	III	16.379
27	Dead	33	Male	79	III	18.1
61	Alive	11.25	Male	71	II	18.629
59	Alive	2.1	Male	80	I	18.801
39	Dead	21	Male	74	III	20.437
9	Dead	12	Male	58	III	20.508
63	Alive	5.28	Female	75	I	20.875
46	Dead	17.5	Male	59	II	21.06
43	Dead	N/A	Female	59	I	21.249
19	Dead	6	Male	59	III	21.357
59	Alive	5	Male	73	II	21.523
60	Alive	6	Female	72	III	22.177
60	Alive	50	Male	73	II	22.685
26	Dead	3.6	Male	61	III	22.847
61	Alive	32	Male	58	III	23.421
24	Dead	33.75	Female	53	III	23.648
61	Alive	6	Female	73	II	24
N/A	Alive	17.5	Male	61	III	24.097
22	Dead	7	Male	76	III	24.263
42	Dead	54	Male	59	III	24.653
59	Alive	20	Female	65	III	24.859
60	Alive	390	Male	63	III	25.729
2	Dead	6	Male	83	II	26.729
59	Alive	45	Male	54	II	26.733
21	Dead	7.2	Male	63	II	26.786
31	Dead	45	Male	53	III	26.825
61	Alive	11.2	Male	63	II	27.257
35	Dead	121.5	Male	58	III	27.288
55	Alive	30	Male	62	III	27.666
62	Alive	9	Male	75	II	28.092
44	Dead	20	Male	65	III	28.511
62	Alive	16	Female	53	II	28.667
62	Alive	24	Male	82	III	29.065
42	Dead	9.45	Male	71	III	29.531
17	Dead	180	Male	65	IV	29.806
61	Alive	20	Male	57	III	29.81
61	Alive	32	Male	79	III	30.207
32	Dead	37.125	Male	59	III	30.217
61	Alive	25	Male	67	II	30.678
10	Dead	40.5	Male	73	III	30.936
60	Alive	5.4	Male	67	II	31.002
63	Alive	27	Female	69	III	32.417
60	Alive	2	Male	45	I	32.589
39	Dead	N/A	Male	69	II	32.65
26	Dead	30	Male	58	III	32.992
59	Alive	N/A	Male	57	II	33.062
28	Dead	8	Female	62	II	33.073
61	Alive	190	Male	55	III	33.177

5	Dead	30	Female	66	III	33.4
11	Dead	16.8	Female	79	III	33.462
35	Dead	3.25	Male	49	III	34.141
60	Alive	40.5	Female	41	II	34.186
5	Dead	35.75	Male	55	III	34.607
15	Dead	37.5	Female	77	II	34.831
6	Dead	49.5	Female	72	III	35.139
37	Dead	66	Male	45	II	35.314
27	Dead	220	Male	59	II	35.502
43	Dead	26	Male	73	II	35.512
1	Dead	42	Female	72	III	36.29
36	Dead	3.75	Male	80	II	36.862
9	Dead	42	Female	68	II	36.901
63	Alive	144	Male	63	II	37.25
11	Dead	117	Male	50	III	37.48
14	Dead	22.5	Male	72	II	37.667
15	Dead	12	Male	78	II	37.838
43	Dead	30	Female	83	III	37.916
58	Dead	91	Male	68	III	38.174
27	Dead	117	Male	80	III	38.288
0	Dead	48	Male	81	III	38.652
2	Dead	63	Male	78	I	38.93
13	Dead	84	Male	62	III	39.875
9	Dead	21	Male	68	III	40.56
11	Dead	32	Male	81	III	40.771
23	Dead	42.25	Male	50	III	42.65
25	Dead	48.75	Female	75	III	42.999
39	Dead	19.25	Male	69	II	44.631
35	Dead	30.375	Male	71	III	46.262
2	Dead	105	Male	63	III	47.239
10	Dead	54.6	Female	65	III	47.838
15	Dead	108	Male	75	IV	49.477
16	Dead	112.5	Male	79	III	51.465
62	Alive	160	Male	47	II	51.675
24	Dead	105	Female	65	III	52.877
34	Dead	180	Female	62	II	53.167
5	Dead	136.5	Male	63	III	54.223
29	Dead	71.5	Male	57	III	57.265
24	Dead	520	Female	34	IV	74.838
28	Dead	250	Female	79	III	81.521

Supplementary Table 2. Protein phosphorylation in gastric cancer cells (yellow color indicates phosphorylation detected)

Protein name	Gene Symbol	Residue	Site Sequence	Gastric cancer cell lines	Phosphorylation frequency (%)
				23132/87 23132/87 AGS AZ-521 FU97 FU97 HCC827 Hs746T IM95 KATO III MKN-1 MKN-45 MKN-45 MKN-45 MKN-74 NCI-H1650 NCI-H1666 NCI-H1703 NCI-H1734 NCI-H1975 NCI-H3255 NCI-H3255 NCI-H358 NUGC-2 NUGC-3 NUGC-4 OCUM-1 RERF-GC-1B SCH SNU-1 SNU-1 SNU-16 SNU-5	
ERK2	MAPK1	Y187-p	HTGFLTEyVATRWYR		100.0
CDK1	CDK1	Y15-p	EKIGEGTyGVVYKGR		97.0
CDK2	CDK2	Y15-p	EKIGEGTyGVVYKAR		93.9
CDK3	CDK3	Y15-p	EKIGEGTyGVVYKAK		93.9
PRP4	PRPF4B	Y849-p	ADNDITPyLVSRFYR		93.9
GSK3A	GSK3A	Y279-p	RGEPNVSyICSRYYR		90.9
GSK3B	GSK3B	Y216-p	RGEPNVSyICSRYYR		90.9
STAT3	STAT3	Y705-p	DPGSAAPyLKTKFIC		90.9
ANXA2	ANXA2	Y24-p	HSTPPSAyGSVKAYT		87.9
P38A	MAPK14	Y182-p	TDDEMTGyVATRWYR		87.9
PTPRA	PTPRA	Y798-p	YIDAFSDyANFK___		87.9
EphA2	EPHA2	Y772-p	EDDPEATyTTSGGKI		84.8
PTTG1IP	PTTG1IP	Y174-p	LFKEENPyARFENN_		84.8
cofilin 1	CFL1	Y140-p	HELQANCyEEVKDRC		81.8
EphA2	EPHA2	Y594-p	TYVDPHTyEDPNQAV		81.8
FAK	PTK2	Y576-p	RYMEDSTyYKASKGK		81.8
Fyn	FYN	Y420-p	RLIEDNEyTARQGAK		81.8
HIPK1	HIPK1	Y352-p	SKAVCSTyLQSRYYR		81.8
HIPK2	HIPK2	Y361-p	SKAVCSTyLQSRYYR		81.8
Lck	LCK	Y394-p	RLIEDNEyTAREGAK		81.8
Src	SRC	Y419-p	RLIEDNEyTARQGAK		81.8
Yes	YES1	Y426-p	RLIEDNEyTARQGAK		81.8
CTNND1	CTNND1	Y904-p	TKSLDNNySTPNERG		78.8
DYRK1A	DYRK1A	Y321-p	LGQRIYQyIQSRFYR		78.8
DYRK1B	DYRK1B	Y273-p	LGQRIYQyIQSRFYR		78.8
GRF-1	ARHGAP3	Y1105-p	RNEEENIySVPHDST		78.8
Lyn	LYN	Y508-p	YTATEGQyQQQP___		78.8
Shc1	SHC1	Y427-p	ELFDDPSyVNVQNLD		78.8
APP	APP	Y757-p	SKMQQNGyENPTYKF		75.8
CD46 iso4	CD46	Y354-p	KADGGAEyATYQTKS		75.8
EGFR	EGFR	Y1197-p	STAENAEyLRVAPQS		75.8
EphA2	EPHA2	Y588-p	QLKPLKTyVDPHTYE		75.8
FAK	PTK2	Y577-p	YMEDSTYyKASKGKL		75.8
Shb	SHB	Y268-p	GKGESAGyMEPYEAQ		75.8
APLP2	APLP2	Y755-p	HGYENPTyKYLEQMQ		72.7
EGFR	EGFR	Y1172-p	ISLDNPDyQQDFFPK		72.7
ERK1	MAPK3	Y204-p	HTGFLTEyVATRWYR		72.7
ITGB1	ITGB1	Y783-p	DTGENPIyKSAVTTV		72.7
JAM-A	F11R	Y280-p	TSSKKVIySQPSARS		72.7
LISCH	LSR	Y551-p	PRSRDPHyDDFRSRE		72.7
Met	MET	Y1234-p	RDMYDKEyYSVHNKT		72.7
plakophilir	PKP4	Y1168-p	GLKSTTNyVDFYSTK		72.7
SgK269	PEAK1	Y635-p	IVINPNAyDNLAIYK		72.7
SHP-2	PTPN11	Y62-p	KIQNTGDyYDLYGGE		72.7
APLP2	APLP2	Y750-p	NKMQNHGyENPTYKY		69.7
ATP1A1	ATP1A1	Y260-p	TARGIVVyTGDRTVM		69.7
cortactin	CTTN	Y421-p	RLPSSPVyEDAASFK		69.7
Erbin	ERBB2IP	Y1104-p	AQIPEGDyLSYREFH		69.7
P130Cas	BCAR1	Y249-p	APGPQDIyDVPPVRG		69.7
STAT3 iso	STAT3	Y704-p	ADPGAAPyLKTKFIC		69.7
cortactin	CTTN	Y446-p	GTEPEPVySMEAADY		66.7
CTNND1	CTNND1	Y228-p	YPGGSDNyGSLSRVT		66.7
Gab1	GAB1	Y659-p	VADERVDyVVVDQQK		66.7
Hck	HCK	Y411-p	RVIEDNEyTAREGAK		66.7
Lyn	LYN	Y397-p	RVIEDNEyTAREGAK		66.7
P130Cas	BCAR1	Y128-p	SKAQQGLyQVPGPSP		66.7
P130Cas	BCAR1	Y234-p	AQPEQDEyDIPRHLL		66.7
Rin1	RIN1	Y36-p	KPAQDPLyDVPNASG		66.7
SHP-2	PTPN11	Y584-p	REDSARVyENVGLMQ		66.7
tensin 3	TNS3	Y780-p	RKLSLGQyDNDAGGQ		66.7

tensin 3	TNS3	Y855-p	PVSPETPyVKTALRH	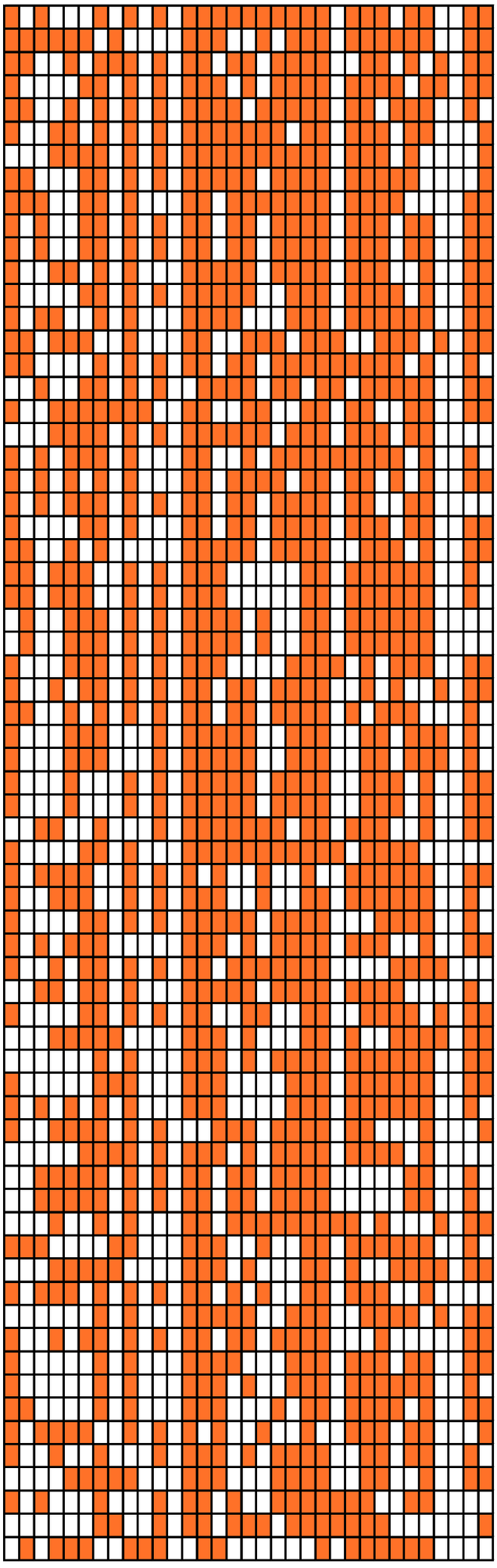	66.7
Yes	YES1	Y537-p	FTATEPQyQPGENL_		66.7
calmodulin	CALM1	Y100-p	FDKDGNGyISAAELR		63.6
CD46 iso4	CD46	Y357-p	GGAEYATyQTKSTTP		63.6
CDK1	CDK1	Y19-p	EGTYGVVyKGRHKTT		63.6
FAK	PTK2	Y397-p	SVSETDDyAEIIDEE		63.6
PIK3R1	PIK3R1	Y467-p	SREYDRLyEEYTRTS		63.6
Shb	SHB	Y114-p	RAMCRLDyCGGSGEP		63.6
Shb	SHB	Y246-p	KVTIADDySDPFDAK		63.6
TAGLN2	TAGLN2	Y192-p	SQAGMTGyGMPRQIL		63.6
TAGLN3	TAGLN3	Y192-p	SQAGMTGyGMPRQIM		63.6
ANXA2	ANXA2	Y30-p	AYGSVKAyTNFDAER		60.6
DDX3	DDX3X	Y104-p	DDRGRSDyDGIGSRG		60.6
Gab1	GAB1	Y406-p	DASSQDCyDIPRAFP		60.6
HIPK3	HIPK3	Y359-p	SKTVCSTyLQSRYYR		60.6
K7	KRT7	Y40-p	GLGSSSLyGLGASRP		60.6
PKCD	PRKCD	Y313-p	SSEPVGIyQGFEKKT		60.6
talin 1	TLN1	Y70-p	EAGKALDyYMLRNGD		60.6
talin 1	TLN1	Y436-p	STVLQQQyNRVGKVE		60.6
ZO2	TJP2	Y1118-p	AQKHPDIyAVPIKTH		60.6
ANXA2	ANXA2	Y238-p	RYKSYSPyDMLESIR		57.6
Cas-L	NEDD9	Y317-p	VGSQNDAyDVPRGVQ		57.6
CTNND1	CTNND1	Y257-p	APSRQDVyGPQPQVR		57.6
DLG3	DLG3	Y673-p	NEVDGQDyHFVVSRE		57.6
DYRK2	DYRK2	Y382-p	EHQRVYTyIQSRFYR		57.6
DYRK4	DYRK4	Y264-p	EHQKVYTyIQSRFYR		57.6
eEF1A1	EEF1A1	Y29-p	TTTGHLIyKCGGIDK		57.6
eEF1A2	EEF1A2	Y29-p	TTTGHLIyKCGGIDK		57.6
EphB4	EPHB4	Y987-p	TGGPAPQy_____		57.6
FLNB	FLNB	Y2502-p	RSSTETCySAIPKAS		57.6
FRK	FRK	Y46-p	QSQRHGHyFVALFDY		57.6
IGF1R	IGF1R	Y1165-p	RDIYETDyYRKGGKG		57.6
InsR	INSR	Y1189-p	RDIYETDyYRKGGKG		57.6
K8	KRT8	Y267-p	IAEVKAQyEDIANRS		57.6
KRT75	KRT75	Y327-p	IAEVKAQyEDIANRS		57.6
N-WASP	WASL	Y256-p	RETSKVIyDFIEKTG		57.6
plakophilin	PKP4	Y478-p	ALNTTATyAEPYRPI		57.6
PXN iso2	PXN	Y118-p	VGEEEHVySFPNKQK		57.6
PZR	MPZL1	Y263-p	NKSESVVyADIRKN_		57.6
SgK223	SGK223	Y411-p	ATQPEPIyAESTKRK		57.6
SKT	KIAA1217	Y393-p	MYRNEGFyADPYLYH		57.6
Tyk2	TYK2	Y292-p	QAEGEPCyIRDSGVA		57.6
ZO2	TJP2	Y426-p	RRHQYSDyDYHSSSE		57.6
EFNB1	EFNB1	Y317-p	ENNYCPHyEKVSGDY		54.5
Fyn	FYN	Y213-p	RKLDNGGyYITTRAQ		54.5
Met	MET	Y1003-p	VSNESVDyRATFPED		54.5
Met	MET	Y1235-p	DMYDKEYySVHNKTG		54.5
MGC1483	C11orf52	Y103-p	HLENATEyATLRFPQ		54.5
PIK3R2	PIK3R2	Y464-p	SREYDQLyEEYTRTS		54.5
PTPRE	PTPRE	Y696-p	FIDIFSDyANFK___		54.5
RPS27	RPS27	Y31-p	LVQSPNSyFMDVKCP		54.5
RPS27L	RPS27L	Y31-p	LVQSPNSyFMDVKCP		54.5
SHIP-2	INPPL1	Y986-p	NSFNNPAyYVLEGVP		54.5
Src	SRC	Y530-p	FTSTEPQyQPGENL_		54.5
Yes	YES1	Y222-p	RKLDNGGyYITTRAQ		54.5
CDK5	CDK5	Y15-p	EKIGEGTyGTVFKAK		51.5
EGFR	EGFR	Y1110-p	GSVQNPVyHNQPLNP		51.5
GRF-1	ARHGAP3	Y1087-p	DGFDPSDyAEPMDAV		51.5
plakophilin	PKP3	Y84-p	RGTSRGQyHTLQAGF		51.5
plakophilin	PKP3	Y176-p	GVGSRADyDTLSLRS		51.5
PLEKHA6	PLEKHA6	Y492-p	PPRSEDIyADPAAYV		51.5
PXN iso2	PXN	Y88-p	PQSSSPVyGSSAKTS		51.5
TBCB	TBCB	Y98-p	SGARLGEyEDVSRVE		51.5
TfR	TFRC	Y20-p	FGGEPLSyTRFSLAR		51.5
Cas-L	NEDD9	Y166-p	RTGHGYVyEYPSRYQ		48.5
caveolin-1	CAV1	Y14-p	VDSEGHLyTVPIREQ		48.5
CDK1	CDK1	T14-p	IEKIGEGtYGVVYKG		48.5

CDK2	CDK2	T14-p	VEKIGEGtYGVVYKA	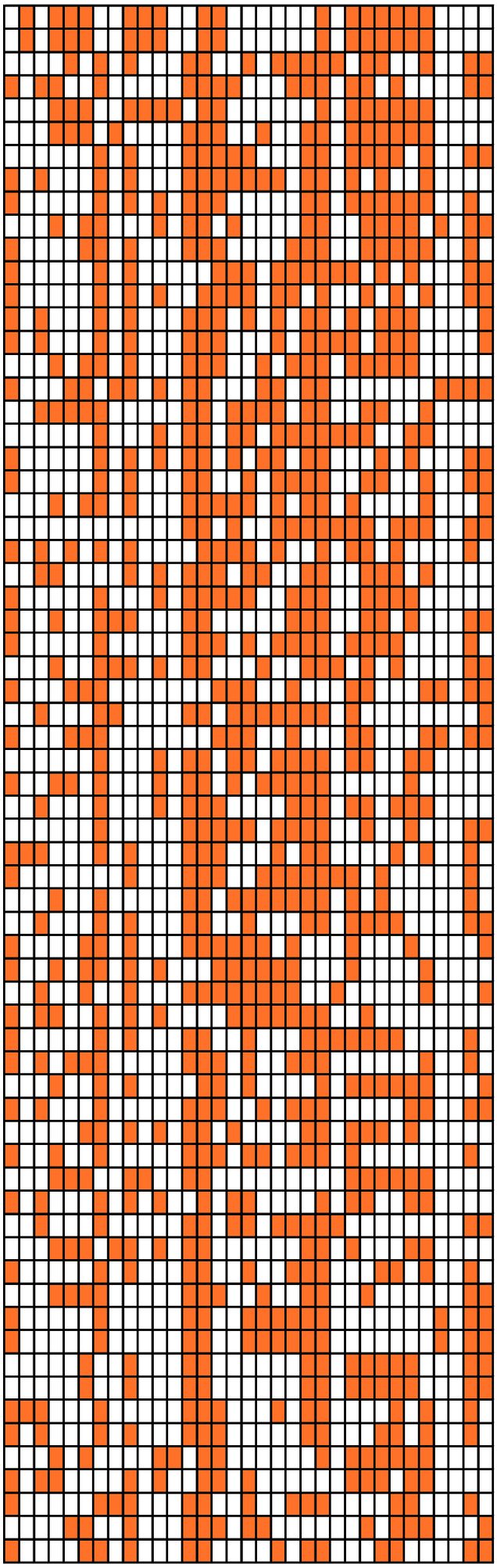	48.5
CDK3	CDK3	T14-p	VEKIGEGtYGVVYKA		48.5
CTNND1	CTNND1	Y96-p	QDHSHLLySTIPRMQ		48.5
EphA2	EPHA2	Y575-p	RQSPEDVyFSKSEQL		48.5
ERK2	MAPK1	T185-p	HDHTGFLtEYVATRW		48.5
Fyn	FYN	Y531-p	FTATEPQyQPGENL_		48.5
ITGB4	ITGB4	Y1207-p	GAQGEGPySSLVSCR		48.5
ITSN2	ITSN2	Y968-p	REEPEALyAAVNKKP		48.5
K19	KRT19	Y391-p	LEGQEDHyNNLSASK		48.5
LDLR	LDLR	Y845-p	ICHNQDGySYPSRQM		48.5
MGC1483	C11orf52	Y78-p	SEDSNLHyADIQVCS		48.5
PAG	PAG1	Y359-p	PSSCNDLyATVKDFE		48.5
PKCD	PRKCD	Y334-p	MQDNSGTyGKIWEGS		48.5
RAIG1	GPRC5A	Y347-p	AHAWPSPyKDYEVKK		48.5
RAIG1	GPRC5A	Y350-p	WPSPYKDyEVKKEGS		48.5
SHIP-2	INPPL1	Y1135-p	KTLSEVDyAPAGPAR		48.5
SLC38A2	SLC38A2	Y41-p	QAALKSHyADVDPEN		48.5
vinculin	VCL	Y822-p	KSFLDSGyRILGAVA		48.5
Cas-L	NEDD9	Y214-p	EIKPQGVyDIPPTKG		45.5
DBNL	DBNL	Y162-p	QAPVGSVyQKTNAVS		45.5
desmoplal	DSP	Y56-p	TDQNSDGyCQTGTMS		45.5
IQGAP1	IQGAP1	Y1510-p	LVKLQQTyAALNSKA		45.5
LISCH	LSR	Y372-p	SAGGQGSyVPLLRDT		45.5
P38D	MAPK13	Y182-p	ADAEMTGyVVTRWYR		45.5
PZR	MPZL1	Y241-p	SHQGPVIyAQLDHSG		45.5
S100A11	S100A11	Y30-p	KYAGKDGyNYTLSKT		45.5
2-Sep	2-Sep	Y17-p	INPETPGyVGFANLP		45.5
Shb	SHB	Y336-p	DDRPADEyDQPWEWN		45.5
syntenin	SDCBP	Y46-p	IPHDGNLyPRLYPEL		45.5
Abl	ABL1	Y393-p	RLMTGDTyTAHAGAK		42.4
Ack	TNK2	Y518-p	GGVKKPTyDPVSEDQ		42.4
Arg	ABL2	Y439-p	RLMTGDTyTAHAGAK		42.4
Cas-L	NEDD9	Y241-p	AGLREKDyDFPPPMR		42.4
CDK2	CDK2	Y19-p	EGTYGVVyKARNKLT		42.4
EFNB2	EFNB2	Y304-p	DSVFCPHyEKVSGDY		42.4
EGFR	EGFR	Y1092-p	TFLPVPEylNQSVPK		42.4
EphB4	EPHB4	Y596-p	VYIDPFTyEDPNEAV		42.4
G6PD	G6PD	Y503-p	MKRVGFQyEGTYKWV		42.4
GIT1	GIT1	Y545-p	ELEDDAIySVHVPAG		42.4
ITGB4	ITGB4	Y1510-p	STTLPRDySTLTSVS		42.4
P130Cas	BCAR1	Y267-p	SQYGQEVyDTPPMAV		42.4
P130Cas	BCAR1	Y287-p	RDPLLEVyDVPPSVE		42.4
P130Cas	BCAR1	Y387-p	RPGPGTLyDVPRERV		42.4
PIK3R2	PIK3R2	Y605-p	KNETEDQyALMEDED		42.4
plakophilir	PKP2	Y166-p	AHYTHSDyQYSQRSQ		42.4
SHANK2	SHANK2	Y989-p	GQMPENPySEVGKIA		42.4
Shc1	SHC1	Y350-p	EPPDHQYyNDFPGKE		42.4
tensin 3	TNS3	Y354-p	GPVDGSLyAKVRKKS		42.4
ANKS1A	ANKS1A	Y455-p	REEDEHPyELLLTAE		39.4
ANXA1	ANXA1	Y39-p	PGSAVSPyPTFNPSS		39.4
ARHGAP1	ARHGAP1	Y243-p	GRPDSPVyANLQELK		39.4
Cas-L	NEDD9	Y345-p	PQERDGVyDVPLHNP		39.4
CDCP1	CDCP1	Y707-p	KGPAVGIyNDNINTE		39.4
Crk	CRK	Y221-p	GGPEPGPyAQPSVNT		39.4
desmoplal	JUP	Y20-p	VTEWQQTyTYDSGIH		39.4
DLG1	DLG1	Y760-p	YEVDGRDyHFVTSRE		39.4
eEF1A1	EEF1A1	Y141-p	REHALLAyTLGVKQL		39.4
eEF1A2	EEF1A2	Y141-p	REHALLAyTLGVKQL		39.4
EFNB1	EFNB1	Y343-p	PQSPANIyYKV____		39.4
EFNB2	EFNB2	Y330-p	PQSPANIyYKV____		39.4
EphB3	EPHB3	Y614-p	VYIDPFTyEDPNEAV		39.4
EphB4	EPHB4	Y774-p	ENSSDPTyTSSLGGK		39.4
ERK1	MAPK3	T202-p	HDHTGFLtEYVATRW		39.4
FAK	PTK2	Y861-p	PIGNQHIyQPVGKPD		39.4
FRK	FRK	Y497-p	YFETDSSySDANNFI		39.4
Fyn	FYN	Y440-p	TAPEAALyGRFTIKS		39.4
GPRC5C	GPRC5C	Y414-p	TLRAEDMySAQSHQA		39.4

HER3	ERBB3	Y1328-p	SAFDNPDyWHSRLFP	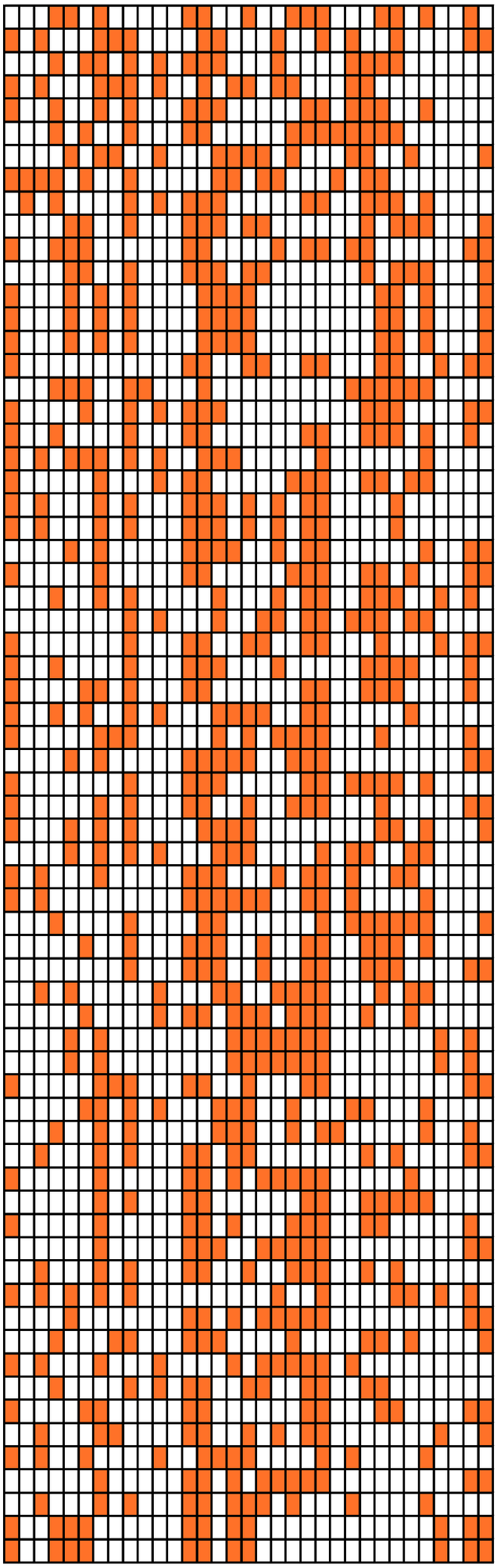	39.4
IRAP	LNPEP	Y70-p	MEEDEEDyESSAKLL		39.4
LIM	PDLIM5	Y251-p	VERYTEFyHVPTHSD		39.4
LPP	LPP	Y317-p	RNDSDPTyGQQGHPN		39.4
plakophilir	PKP4	Y415-p	DLHITPIyEGRTYYS		39.4
plakophilir	PKP4	Y1115-p	RLQHQQLyYSQDDSN		39.4
PTRF	PTRF	Y308-p	FTPDHVVyARSKTAV		39.4
RIPK2	RIPK2	Y381-p	SRKAQDCyFMKLHHC		39.4
RPS10	RPS10	Y12-p	KKNRIAIyELLFKEG		39.4
Src	SRC	Y439-p	TAPEAALyGRFTIKS		39.4
VASP	VASP	Y39-p	AFSRVQIyHNPTANS		39.4
Yes	YES1	Y446-p	TAPEAALyGRFTIKS		39.4
ACTA1	ACTA1	Y93-p	KIWHHTFyNELRVAP		36.4
ACTB	ACTB	Y91-p	KIWHHTFyNELRVAP		36.4
ACTG1	ACTG1	Y91-p	KIWHHTFyNELRVAP		36.4
APP	APP	Y762-p	NGYENPTyKFFEQMQ		36.4
ARHGAP:	ARHGAP1	S240-p	PNQGRPDsPVYANLQ		36.4
ATP1A1	ATP1A1	Y10-p	KGVGRDKyEPAAVSE		36.4
Bcr	BCR	Y177-p	ADAEKPFyVNVEFHH		36.4
CdkL5	CDKL5	Y171-p	NNANYTEyVATRWYR		36.4
CDV-3	CDV3	Y244-p	KLQLDNQyAVLENQK		36.4
cofilin 1	CFL1	Y89-p	YALYDATyETKESKK		36.4
cofilin 2	CFL2	Y89-p	YALYDATyETKESKK		36.4
CTNNA1	CTNNA1	Y177-p	EQDLGIQyKALKPEV		36.4
CTNND1	CTNND1	Y174-p	ASSVSNNyIQTLGRD		36.4
DNAJA1	DNAJA1	Y381-p	RHYNGEAyEDDEHHP		36.4
FAK	PTK2	Y407-p	IIDEEDTyTMPSTRD		36.4
Hrs	HGS	Y216-p	VRVCEPCyEQLNRKA		36.4
IRS2	IRS2	Y823-p	CGGDSDQyVLMSSPV		36.4
occludin	OCLN	Y315-p	VPSPPSDyVERVDSP		36.4
P130Cas	BCAR1	Y306-p	PSNHHAVyDVPPSVS		36.4
PAG	PAG1	Y417-p	LVPKENDyESISDLQ		36.4
PAR3-alpl	PARD3	Y388-p	RFSPDSQyIDNRSVN		36.4
plakophilir	PKP2	Y168-p	YTHSDYQySQRSQAG		36.4
plakophilir	PKP3	Y195-p	PGGLDDRySLVSEQL		36.4
POTEF	POTEF	Y791-p	KIWHHTFyNELRVAP		36.4
Pyk2	PTK2B	Y579-p	RYIEDEDyYKASVTR		36.4
RAIG1	GPRC5A	Y317-p	EETGDTLyAPYSTHF		36.4
SgK269	PEAK1	Y641-p	AYDNLAIyKSFLGTS		36.4
Shc1	SHC1	Y349-p	EEPPDHQyYNDFPGK		36.4
SHIP-2	INPPL1	Y886-p	LGTRERLyEWISIDK		36.4
SLC1A5	SLC1A5	Y524-p	GNPLLKHyRGPAGDA		36.4
tensin 1	TNS1	Y1404-p	RAGSLPNyATINGKV		36.4
tensin 3	TNS3	Y601-p	QMVVAHQySFAPDGE		36.4
ACTB	ACTB	Y198-p	KILTERGySFTTTAE		33.3
ACTG1	ACTG1	Y198-p	KILTERGySFTTTAE		33.3
ANK3	ANK3	Y533-p	NAATTSGyTPLHLSA		33.3
BCAR3	BCAR3	Y266-p	LRCLEEHyGTSPGQA		33.3
BCS1L	BCS1L	Y181-p	SEWRPFGyPRRRRPL		33.3
CDCP1	CDCP1	Y806-p	PESESEPyTFSHPNN		33.3
CDK3	CDK3	Y19-p	EGTYGVVyKAKNRET		33.3
CTNND1	CTNND1	Y248-p	YRPSMEGyRAPSRQD		33.3
CTNND1	CTNND1	Y334-p	EEVPSDQyYWAPLAQ		33.3
ENO1	ENO1	Y287-p	YKSFIKDyPVVSIED		33.3
EphB2	EPHB2	Y780-p	DDTSDPTyTSALGGK		33.3
ERK5	MAPK7	Y221-p	HQYFMTEyVATRWYR		33.3
Fyn	FYN	Y214-p	KLDNGGYyITTRAQF		33.3
Gab1	GAB1	Y259-p	ASVDSSLyNLPRSYS		33.3
GIT2	GIT2	Y592-p	NSTPESDyDNTPNDM		33.3
JAK2	JAK2	Y570-p	VRREVGDyGQLHETE		33.3
LAMTOR:	LAMTOR1	Y40-p	LNGAEPNyHSLPSAR		33.3
LDH-A	LDHA	Y239-p	KQVVESAyEVIKLKG		33.3
LPP	LPP	Y301-p	GRYYEGYyAAGPGYG		33.3
MIG-6	ERRFI1	Y395-p	KVSSTHYyLLPERPP		33.3
P130Cas	BCAR1	Y327-p	PLLREETyDVPPAFA		33.3
PGAM1	PGAM1	Y92-p	WRLNERHyGGLTGLN		33.3
PGAM2	PGAM2	Y92-p	WRLNERHyGGLTGLN		33.3

PIK3R3	PIK3R3	Y199-p	SKEYDRLyEEYTRTS	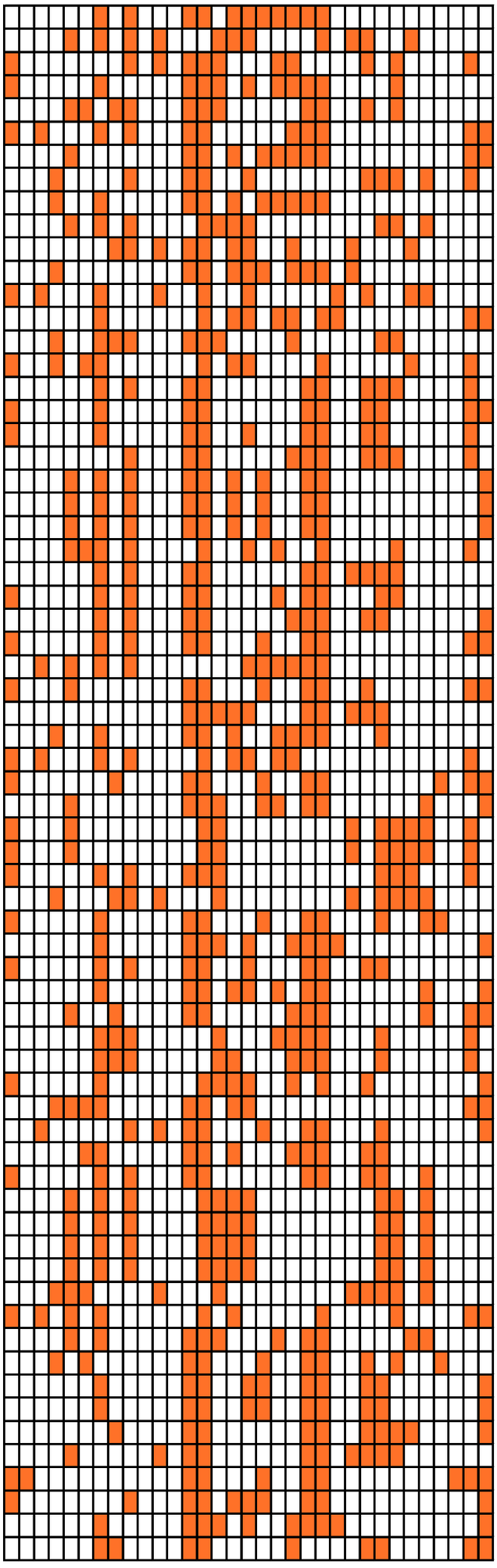	33.3
Pyk2	PTK2B	Y580-p	YIEDEDYyKASVTRL		33.3
RBM3	RBM3	Y155-p	GGNYRDNyDN_____		33.3
Syk	SYK	Y323-p	STVSFNPyEPELAPW		33.3
syndecan-	SDC1	Y309-p	PTKQEEFyA_____		33.3
tensin 3	TNS3	Y333-p	PLIRWDSyENLSADG		33.3
Yes	YES1	Y223-p	KLDNGGYyITTRAQF		33.3
Abi-1	ABI1	Y213-p	PPTVPNDyMTSPARL		30.3
Ack	TNK2	Y859-p	KKVSSTHyYLLPERP		30.3
ACTC1	ACTC1	Y93-p	KIWHHTFyNELRVAP		30.3
AFAP1L2	AFAP1L2	Y413-p	DPSPDHLySFRILHK		30.3
ANXA1	ANXA1	Y207-p	DSDARALyEAGERRK		30.3
Cas-L	NEDD9	Y92-p	TFGQQKLyQVPNPQA		30.3
CASKIN2	CASKIN2	Y253-p	DVNIRNTyNQTALDI		30.3
Cbl	CBL	Y700-p	EGEEDTEyMTPSSRP		30.3
CDV-3	CDV3	Y190-p	PQGPPEIySDTQFPS		30.3
claudin 3	CLDN3	Y219-p	TGYDRKDyV_____		30.3
CTNND1	CTNND1	Y296-p	MGYDDLDyGMMSDYG		30.3
DDX3	DDX3X	Y69-p	SSKDKDAySSFGSRS		30.3
EHM2 iso	EPB41L4E	Y493-p	GDDSHFDyVHDQNQK		30.3
ENO1	ENO1	Y44-p	SGASTGIyEALELRD		30.3
ENO2	ENO2	Y44-p	SGASTGIyEALELRD		30.3
ENO3	ENO3	Y44-p	SGASTGIyEALELRD		30.3
EphA1	EPHA1	Y781-p	LDDFDGTyETQGGKI		30.3
EPS8	EPS8	Y525-p	NRHIDRNyEPLKTQP		30.3
EPS8	EPS8	Y774-p	CPEGARVySQITVQK		30.3
Erbin	ERBB2IP	Y1164-p	MSVSDFNySRTSPSK		30.3
ESYT1	ESYT1	Y822-p	GTKHLSPyATLTVGD		30.3
Fer	FER	Y402-p	EPPPVVNyEEDARSV		30.3
FLOT1	FLOT1	Y203-p	QEKVSAQyLSEIEMA		30.3
G6PD	G6PD	Y507-p	GFQYEGTyKWVNPHK		30.3
HER2	ERBB2	Y1248-p	PTAENPEyLGLDVPV		30.3
hnRNP A2	HNRNPA2	Y336-p	GPYGGGNyGPGGSGG		30.3
Hrs	HGS	Y132-p	YKVVQDTyQIMKVEG		30.3
HSP90B	HSP90AB	Y484-p	KETQKSIyYITGESK		30.3
IGF1R	IGF1R	Y1161-p	FGMTRDIyETDYYRK		30.3
InsR	INSR	Y1185-p	FGMTRDIyETDYYRK		30.3
IRS2	IRS2	Y742-p	SSPEDSGyMRMWCGS		30.3
Lasp-1	LASP1	Y171-p	IPTSAPVyQQPQQQP		30.3
LDH-B	LDHB	Y240-p	KMVVESAyEVIKLKG		30.3
Mer	MERTK	Y753-p	KKIYSGDyYRQGRIA		30.3
MINK	MINK1	Y906-p	LHADSNGyTNLPDVV		30.3
Nck1	NCK1	Y105-p	VDPGERLyDLNMPAY		30.3
NRP1	NRP1	Y920-p	KLNTQSTySEA____		30.3
PAG	PAG1	Y317-p	EEEISAMySSVNKPG		30.3
PAG	PAG1	Y341-p	LTVPESTyTSIQGDP		30.3
PAR3-alp	PARD3	Y719-p	RRISHSLySGIEGLD		30.3
PGAM1	PGAM1	Y26-p	ENRFSGWyDADLSPA		30.3
PIK3R1	PIK3R1	Y607-p	NENTEDQySLVEDDE		30.3
plakophilir	PKP4	Y157-p	NSYSDSGyQEAGSFH		30.3
plakophilir	PKP4	Y372-p	GQQQYDIyERMVPPR		30.3
POTE2	POTEE	Y791-p	KIWHHTFyNELRVAP		30.3
POTEI	POTEI	Y791-p	KIWHHTFyNELRVAP		30.3
POTEJ	POTEJ	Y754-p	KIWHHTFyNELRVAP		30.3
POTEM is	POTEM	Y8-p	KIWHHTFyNELRVAP		30.3
PXN iso2	PXN	S85-p	HQQPQSSsPVYGSSA		30.3
S100A10	S100A10	Y25-p	KFAGDKGyLTKEDLR		30.3
SKT	KIAA1217	Y244-p	KDESRNVyYELNDVR		30.3
SPRY4	SPRY4	Y52-p	TSHVENDyIDNPSLA		30.3
STAT5A	STAT5A	Y694-p	LAKAVDGyVKPQIKQ		30.3
STAT5B	STAT5B	Y699-p	TAKAVDGyVKPQIKQ		30.3
STX4	STX4	Y115-p	KEEADENyNSVNTRM		30.3
syndecan-	SDC4	Y197-p	KAPTNEFyA_____		30.3
TKT	TKT	Y275-p	EQIIQEIySQIQSKK		30.3
TMEM106	TMEM106	Y50-p	GDVSQFPyVEFTGRD		30.3
Tyro3	TYRO3	Y685-p	RKIYSGDyYRQGCAS		30.3
Abi-1	ABI1	Y198-p	TLGRNTPyKTLEPVK		27.3

ACTA1	ACTA1	Y55-p	GMGQKDSyVGDEAQS	27.3
ACTA2	ACTA2	Y55-p	GMGQKDSyVGDEAQS	27.3
ACTB	ACTB	Y53-p	GMGQKDSyVGDEAQS	27.3
ACTG1	ACTG1	Y53-p	GMGQKDSyVGDEAQS	27.3
ACTG2	ACTG2	Y54-p	GMGQKDSyVGDEAQS	27.3
ACTN1	ACTN1	Y246-p	MTYVSSFyHAFSGAQ	27.3
ACTN4	ACTN4	Y265-p	MTYVSSFyHAFSGAQ	27.3
ALDOA	ALDOA	Y3-p	_____MPyQYPALTP	27.3
ANXA2	ANXA2	Y316-p	RKYGKSLyYYIQQDT	27.3
CALM2	CALM2	Y100-p	FDKDGNGyISAAELR	27.3
CALM3	CALM3	Y100-p	FDKDGNGyISAAELR	27.3
CrkL	CRKL	Y251-p	QKRVPCAyDKTALAL	27.3
CTNND1	CTNND1	Y280-p	HRFHPEPyGLEDDQR	27.3
Dok1	DOK1	Y449-p	KSHNSALySQVQKSG	27.3
DYRK1A	DYRK1A	Y145-p	DGYDDDNyDYIVKNG	27.3
EFNB1	EFNB1	Y329-p	GDYGHPVyIVQEMPP	27.3
EFNB2	EFNB2	Y316-p	GDYGHPVyIVQEMPP	27.3
EPB41L1	EPB41L1	Y343-p	IKIRPGEyEQFESTI	27.3
EphB3	EPHB3	Y608-p	IAPGMKVyIDPFTYE	27.3
EphB4	EPHB4	Y590-p	IGHGTKVyIDPFTYE	27.3
EPS8	EPS8	Y485-p	EHSSVSEyHPADGYA	27.3
EPS8	EPS8	Y491-p	EYHPADGyAFSSNIY	27.3
FRS2	FRS2	Y306-p	PSVNKLVyENINGLS	27.3
HER2	ERBB2	Y877-p	LDIDETEyHADGGKV	27.3
hnRNP A:	HNRNPA3	Y360-p	GRSSGSPyGGGYGSG	27.3
IRSp53	BAIAP2	Y337-p	QSKLSDSySNTLPVR	27.3
ITGB1	ITGB1	Y795-p	TTVVNPKyEGK____	27.3
JNK2	MAPK9	Y185-p	TNFMMTPyVVTRYYR	27.3
K8	KRT8	Y25-p	RAFSSRSyTSGPGSR	27.3
K8	KRT8	Y282-p	RAEAESMyQIKYEEL	27.3
LAPTM4A	LAPTM4A	Y230-p	EKEPPPPyLPA____	27.3
LISCH	LSR	Y406-p	DDSMRVLyYMEKELA	27.3
Met	MET	Y1365-p	NVKCVAPyPSLLSSE	27.3
MYH9	MYH9	Y1408-p	HEEKVAAyDKLEKTK	27.3
PAR3-alpl	PARD3	Y1080-p	RQARERDyAEIQDFH	27.3
plakophilir	PKP4	Y420-p	PIYEGRTyYSPVYRS	27.3
PLCG1	PLCG1	Y771-p	IGTAEPDyGALYEGR	27.3
PLCG1	PLCG1	Y783-p	EGRNPGFyVEANPMP	27.3
PXN	PXN	Y118-p	VGEEEHVySFPNKQK	27.3
PYGB	PYGB	Y197-p	WEKARPEyMLPVHFY	27.3
RABL6	RABL6	Y726-p	RHPGGGDyEEL____	27.3
RAIG1	GPRC5A	Y320-p	GDTLYAPySTHFQLQ	27.3
RPLP0	RPLP0	Y24-p	IIQLLDDyPKCFIVG	27.3
7-Sep	7-Sep	Y319-p	RKLAAVTyNGVDNNK	27.3
9-Sep	9-Sep	Y278-p	KAPVDFGyVGIDSIL	27.3
SHP-1	PTPN6	Y564-p	SKHKEDVyENLHTKN	27.3
snRNP 7(	SNRNP70	Y126-p	LRREFEVyGPIKRIH	27.3
SPRY1	SPRY1	Y53-p	AIRGSNEyTEGPSVV	27.3
ZNF185	ZNF185	Y408-p	PKGALADyEGKDVAT	27.3
ZO1	TJP1	Y1066-p	YRYESSSyTDQFSRN	27.3
abLIM	ABLIM1	Y461-p	GSINSPVySRHSYTP	24.2
ACTC1	ACTC1	Y55-p	GMGQKDSyVGDEAQS	24.2
ADAM9	ADAM9	Y769-p	PPREVPIyANRFAVP	24.2
ADAM9	ADAM9	Y815-p	PAPAPPLySSLT___	24.2
afadin	MLLT4	Y1497-p	IERRDLQyITVSKEE	24.2
ARHGAP!	ARHGAP5	Y1109-p	KGYSDEIyVVPDDSQ	24.2
ATP1A1	ATP1A1	Y542-p	KDAFQNAyLELGGLG	24.2
Brk	PTK6	Y447-p	RLSSFTSyENPT___	24.2
C6orf132	C6orf132	Y1142-p	KAPGSADyGFAPAAG	24.2
Cas-L	NEDD9	Y189-p	SHTTQGVyDIPPSSA	24.2
CCT-theta	CCT8	Y30-p	SGLEEAVyRNIQACK	24.2
cortactin	CTTN	Y334-p	VTQVSSAyQKTVPVE	24.2
cortactin	CTTN	Y453-p	YSMEAADyREASSQQ	24.2
cortactin i	CTTN	Y265-p	LHESQKDySKGFGGK	24.2
CrkL	CRKL	Y198-p	GNRNSNSyGIPEPAH	24.2
CTNND1	CTNND1	Y193-p	GNGGPGPyVGQAGTA	24.2
CTNND1	CTNND1	S252-p	MEGYRAPsRQDVYGP	24.2

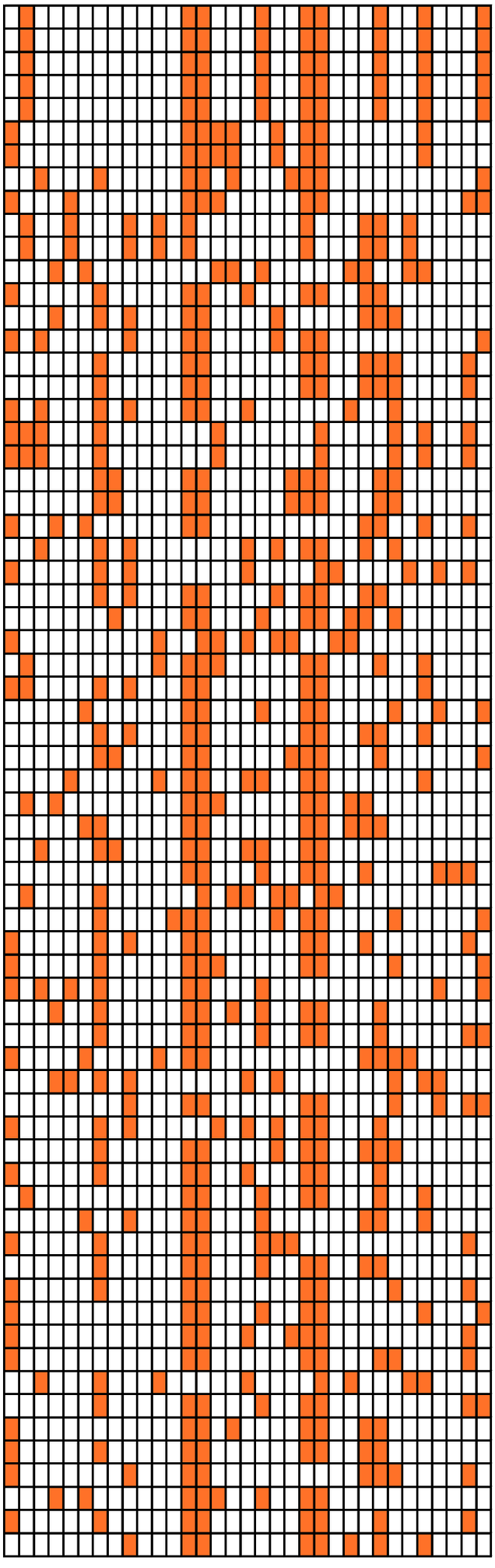

CTNND1	CTNND1	Y335-p	EVPSDQYyWAPLAQH	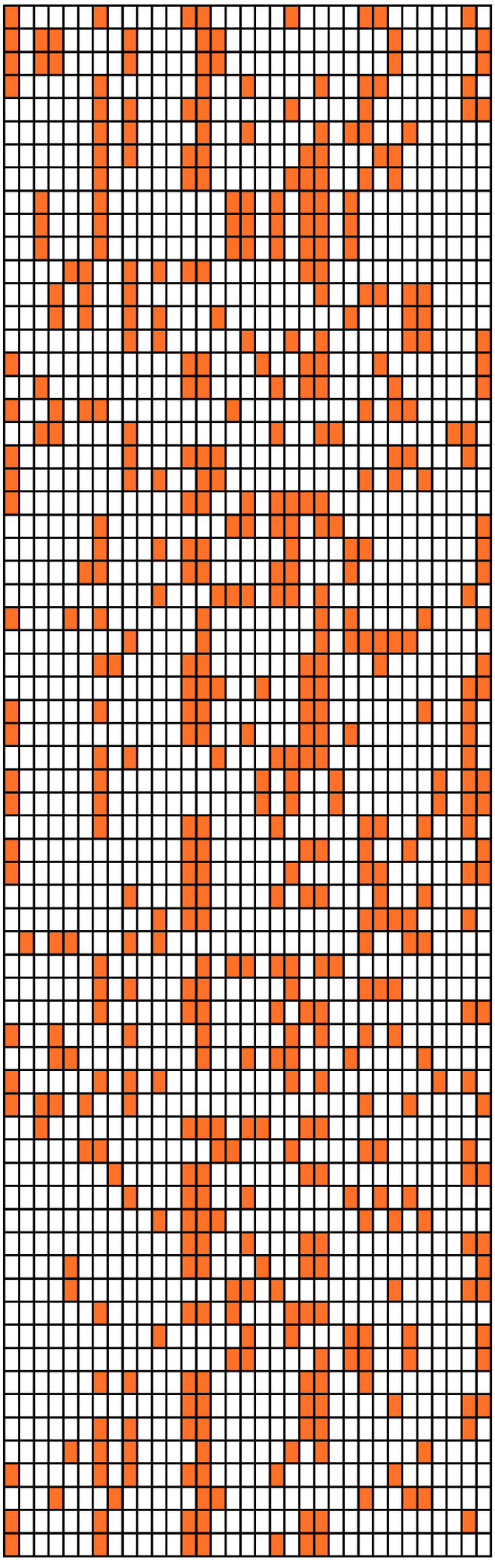	24.2
CYFIP1	CYFIP1	Y108-p	QPNRVEIyEKTVEVL		24.2
CYFIP2	CYFIP2	Y108-p	QPNRVEIyEKTVEVL		24.2
DDX3Y	DDX3Y	Y69-p	CSKDKDAySSFGSRD		24.2
desmogle	DSG2	Y1013-p	QHLQDVPyVMVRERE		24.2
EGFR	EGFR	Y869-p	LGAEEKEyHAEGGKV		24.2
EPB41	EPB41	Y660-p	RLDGENIyIRHSNLM		24.2
EPB41L1	EPB41L1	Y864-p	LVTKAVVyRETDPSP		24.2
EphA3	EPHA3	Y779-p	EDDPEAAyTTRGGKI		24.2
EphA4	EPHA4	Y779-p	EDDPEAAyTTRGGKI		24.2
EphA5	EPHA5	Y833-p	EDDPEAAyTTRGGKI		24.2
EphB4	EPHB4	Y574-p	SNGREAEySDKHGQY		24.2
FAK	PTK2	T575-p	SRYMEDStYYKASKG		24.2
FCHSD2	FCHSD2	Y659-p	SLPPLPLyDQPPSSP		24.2
Fer	FER	Y714-p	RQEDGGVySSSGLKQ		24.2
G6PD	G6PD	Y401-p	VQPNEAVyTKMMTKK		24.2
GPRC5C	GPRC5C	Y387-p	KVPSEGAyDIILPRA		24.2
hnRNP A(	HNRNPA(	Y180-p	AVPKEDIySGGGGGG		24.2
hnRNP A:	HNRNPA1	Y347-p	PYGGGGQyFAKPRNQ		24.2
IRS2	IRS2	Y653-p	NLGADDGyMPMTPGA		24.2
K18	KRT18	Y36-p	VSSAASVyAGAGGSG		24.2
K7	KRT7	Y205-p	KKDVDAAyMSKVELE		24.2
KIAA0020	KIAA0020	Y259-p	SAIVEYAyNDKAILE		24.2
KIRREL	KIRREL	Y721-p	SGLERTPyEAYDPIG		24.2
KIRREL	KIRREL	Y724-p	ERTPYEAyDPIGKYA		24.2
Lyn	LYN	Y193-p	RSLDNGGyYISPRIT		24.2
Lyn	LYN	Y194-p	SLDNGGYyISPRITF		24.2
Met	MET	S1236-p	MYDKEYYsVHNKTGA		24.2
Met	MET	Y1356-p	YVHVNATyVNVKCVA		24.2
MIG-6	ERRFI1	Y394-p	KKVSSTHyYLLPERP		24.2
MPP5	MPP5	Y243-p	PITDERVyESIGQYG		24.2
nectin 1	PVRL1	Y468-p	DEDAKRPyFTVDEAE		24.2
occludin	OCLN	Y287-p	LWDKEHIyDEQPPNV		24.2
PDHA1	PDHA1	Y301-p	MSDPGVSyRTREEIQ		24.2
PDHA2	PDHA2	Y299-p	MSDPGVSyRTREEIQ		24.2
plakophilir	PKP3	Y210-p	EPAATSTyRAFAYER		24.2
plakophilir	PKP3	Y390-p	GAMRNLIyDNADNKL		24.2
plakophilir	PKP4	Y306-p	PNGPTPQyQTTARVG		24.2
PLEKHA7	PLEKHA7	Y656-p	GKSADDTyLQLKKDL		24.2
PPP1R11	PPP1R11	Y64-p	SSKCCCIyEKPRAFG		24.2
PRP4	PRPF4B	S852-p	DITPYLVsRFYRAPE		24.2
PXN	PXN	Y88-p	PQSSSPVyGSSAKTS		24.2
Ron	MST1R	Y1238-p	RDILDREyYSVQQHR		24.2
RPSA	RPSA	Y139-p	QPLTEASyVNLPTIA		24.2
SLC7A11	SLC7A11	Y15-p	STISKGGyLQGNVNG		24.2
talin 1	TLN1	Y26-p	FEPSTMVyDACRIIR		24.2
YB-1	YBX1	Y162-p	PRNYQQNyQNSESGE		24.2
Yes	YES1	Y32-p	VSTSVSHyGAEPTTV		24.2
Yes	YES1	Y194-p	SETTKGAySLSIRDW		24.2
ZO2	TJP2	Y1007-p	TQNKEESyDFSKSYE		24.2
ACP1	ACP1	Y132-p	QLIIEDPyYGNDSDF		21.2
AFAP1L2	AFAP1L2	Y54-p	SSSSDEEyIYMNKVT		21.2
AHNAK	AHNAK	Y715-p	GTKVKGEyDVTVPKL		21.2
ALDOA	ALDOA	Y5-p	___MPYQyPALTPEQ		21.2
ANXA11	ANXA11	Y482-p	RMYGKSLyHDISGDT		21.2
ANXA2	ANXA2	Y317-p	KYGKSLYyYIQQDTK		21.2
ARHGEF5	ARHGEF5	Y656-p	DRRSGRDySTVSASP		21.2
Axl	AXL	Y702-p	KKIYNGDyYRQGRIA		21.2
Axl	AXL	Y703-p	KIYNGDYyRQGRIAK		21.2
BAG3	BAG3	Y247-p	YQTHQPVyHKIQGDD		21.2
claudin 1	CLDN1	Y210-p	APSSGKDyV_____		21.2
claudin 3	CLDN3	Y214-p	GASLGTGyDRKDYV_		21.2
CLTC	CLTC	Y634-p	LEHFTDLyDIKRAVV		21.2
cofilin 1	CFL1	Y68-p	GQTVDDPyATFVKML		21.2
CrkL	CRKL	Y207-p	IPEPAHAyAQPQTTT		21.2
CTNNB1	CTNNB1	Y30-p	SHWQQQSyLDSGIHS		21.2
CTNND1	CTNND1	Y221-p	SRHYEDGyPGGSDNY		21.2

CTNND1	CTNND1	S230-p	GGSDNYGsLSRVTRI	21.2
CTNND1	CTNND1	Y302-p	DYGMMSDyGTARRTG	21.2
CXADR	CXADR	Y318-p	EGYSKTQyNQVPSED	21.2
DCBLD2	DCBLD2	Y732-p	CSSAQAQyDTPKAGK	21.2
DCBLD2	DCBLD2	Y750-p	PAPDELVyQVPQSTQ	21.2
DOCK1	DOCK1	Y1811-p	LKGSVADyGNLMENQ	21.2
EFNB1	EFNB1	Y313-p	LRTTENNyCPHYEKV	21.2
EGFR	EGFR	Y727-p	SGAFGTVyKGLWIPE	21.2
EGFR	EGFR	Y998-p	SPTDSNFyRALMDEE	21.2
EPB41L2	EPB41L2	Y623-p	RVEGDNIyVRHSNLM	21.2
EphB1	EPHB1	Y600-p	IYIDPFTyEDPNEAV	21.2
EphB2	EPHB2	Y602-p	IYIDPFTyEDPNEAV	21.2
EphB3	EPHB3	Y792-p	DDPSDPTyTSSLGGK	21.2
Erbin	ERBB2IP	Y884-p	EIGGLKIyDILSDNG	21.2
ERP29	ERP29	Y66-p	KFDTQYPyGEKQDEF	21.2
FAK	PTK2	Y570-p	GDFGLSRyMEDSTYY	21.2
Fgr	FGR	Y180-p	SETTKGAySLSIRDW	21.2
Fyn	FYN	Y185-p	SETTKGAySLSIRDW	21.2
GDI2	GDI2	Y203-p	DYLDQPCyETINRIK	21.2
GSK3A	GSK3A	S278-p	VRGEPNVsYICSRYY	21.2
GSK3B	GSK3B	S215-p	VRGEPNVsYICSRYY	21.2
HER2	ERBB2	Y735-p	SGAFGTVyKGIWIPD	21.2
HER3	ERBB3	Y1289-p	CPASEQGyEEMRAFQ	21.2
HER3	ERBB3	Y1307-p	HQAPHVHyARLKTLR	21.2
HER4	ERBB4	Y733-p	SGAFGTVyKGIWVPE	21.2
hnRNP A:	HNRNPA1	Y341-p	GGRSSGPyGGGGQYF	21.2
hnRNP A:	HNRNPA1	Y357-p	KPRNQGGyGGSSSSS	21.2
HSPC227	PDZD11	Y10-p	SRIPYDDyPVVFLPA	21.2
IRTKS	BAIAP2L1	Y274-p	SNVVRKDyDTLSKCS	21.2
ITSN2	ITSN2	Y553-p	EYQNKLIyLVPEKQL	21.2
K7	KRT7	S38-p	PGGLGSSsLYGLGAS	21.2
K8	KRT8	S24-p	PRAFSSRsYTSGPGS	21.2
KLC2	KLC2	Y345-p	GKAEEVEyYYRRALE	21.2
Lck	LCK	Y505-p	FTATEGQyQPQP___	21.2
LDLR	LDLR	Y828-p	INFDNPVyQKTTEDE	21.2
LDLR	LDLR	Y847-p	HNQDGYSyPSRQMVS	21.2
LMBRD2	LMBRD2	Y290-p	MGRNMDDyEDFDEKH	21.2
LPP	LPP	Y300-p	QGRYYEGyYAAGPGY	21.2
Lyn	LYN	Y316-p	VTREEPIyIITEYMA	21.2
MUC1	MUC1	Y1229-p	SSTDRSPyEKVSAGN	21.2
MYO10	MYO10	Y1128-p	YRCSVGTyNSSGAYR	21.2
MYO1E	MYO1E	Y989-p	RSNQKSLyTSMARPP	21.2
nectin 4	PVRL4	Y502-p	KPTGNGIyINGRGHL	21.2
PAR3-alp	PARD3	Y489-p	IGGSAPIyVKNILPR	21.2
PDHA1	PDHA1	Y289-p	MELQTYRyHGHSMSD	21.2
PDHA2	PDHA2	Y287-p	MELQTYRyHGHSMSD	21.2
PGAM4	PGAM4	Y92-p	WRLNERHyGGLTGLN	21.2
plakophilir	PKP4	Y421-p	IYEGRTYySPVYRSP	21.2
plakophilir	PKP4	Y470-p	LTYQRNNyALNTTAT	21.2
PLEKHA7	PLEKHA7	Y470-p	SLSFPENyQTLPKST	21.2
profilin 1	PFN1	Y129-p	GLINKKCyEMASHLR	21.2
PSMA2	PSMA2	Y76-p	TKHIGLVySGMGPDY	21.2
PXN iso2	PXN	Y31-p	FLSEETPySYPTGNH	21.2
SLC38A2	SLC38A2	Y28-p	SSNSDFNySYPTKQA	21.2
SLC6A8	SLC6A8	Y11-p	KSAENGIySVSGDEK	21.2
SPRY2	SPRY2	Y55-p	AIRNTNEyTEGPTVV	21.2
tensin 3	TNS3	S332-p	DPLIRWDsYENLSAD	21.2
WIRE	WIPF2	Y74-p	PKGSSGGyGSGGAAL	21.2
zyxin	ZYX	Y316-p	PQPPSFTyAQQREKP	21.2
A6	TWF1	Y309-p	ELTADFLyEEVHPKQ	18.2
abLIM	ABLIM1	Y357-p	RTSSESIySRPGSSI	18.2
Ack	TNK2	Y284-p	LPQNDDHyVMQEHRK	18.2
AHNAK	AHNAK	Y964-p	GPKVKGEyDMTVPKL	18.2
ANXA2	ANXA2	Y188-p	EDGSVIDyELIDQDA	18.2
ANXA5	ANXA5	Y94-p	PSRLYDAyELKHALK	18.2
ARHGAP!	ARHGAP5	Y1091-p	DMDPSDNyAEPIDTI	18.2
ARPP-19	ARPP19	Y65-p	KYFDSGDyNMAKAKM	18.2